3-comp. modelling of C-rich AGB star winds V. Effects of freq.-dep. rad. transfer including drift

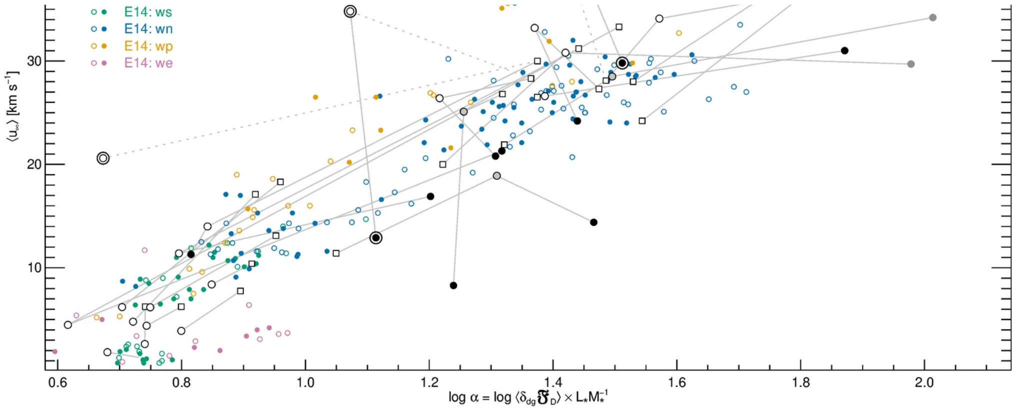

Christer Sandin

Collaborator: Lars Mattsson

NORDITA

Nordita Astrophysics seminars, Nordita, 2020-11-25; 13:30–14:30

This talk is about the results of our latest publication on the modeling of the extended stellar atmosphere and mass loss from low- to intermediate-mass asymptotic giant branch (AGB) stars.

Here, we delve into the topic using frequency-dependent opacities and a higher numerical accuracy than before.

As it turns out, everything changes!

I have done this work in my free time, beginning in about May 2018. I had an opportunity to finish the work and submit the paper while I was a researcher at Nordita in the spring of 2020.

NORDITA

Monthly Notices of the ROYAL ASTRONOMICAL SOCIETY
MNRAS **499,** 1531–1560 (2020) doi:10.1093/mnras/staa2714

Three-component modelling of C-rich AGB star winds – V. Effects of frequency-dependent radiative transfer including drift★

Christer Sandin and Lars Mattsson
Nordita, KTH Royal Institute of Technology and Stockholm University, Roslagstullsbacken 23, SE-106 91 Stockholm, Sweden

Accepted 2020 September 1. Received 2020 September 1; in original form 2020 June 19

ABSTRACT
Stellar winds of cool carbon stars enrich the interstellar medium with significant amounts of carbon and dust. We present a study of the influence of two-fluid flow on winds where we add descriptions of frequency-dependent radiative transfer (RT). Our radiation hydrodynamic models in addition include stellar pulsations, grain growth and ablation, gas-to-dust drift using one mean grain size, dust extinction based on both the small particle limit (SPL) and Mie scattering, and an accurate numerical scheme. We calculate models at high spatial resolution using 1024 gridpoints and solar metallicities at 319 frequencies, and we discern effects of drift by comparing drift models to non-drift models. Our results show differences of up to 1000 per cent in comparison to extant results. Mass-loss rates and wind velocities of drift models are typically, but not always, lower than in non-drift models. Differences are larger when Mie scattering is used instead of the SPL. Amongst other properties, the mass-loss rates of the gas and dust, dust-to-gas density ratio, and wind velocity show an exponential dependence on the dust-to-gas speed ratio. Yields of dust in the least massive winds increase by a factor 4 when drift is used. We find drift velocities in the range 10–67 $km\,s^{-1}$, which is drastically higher than in our earlier works that use grey RT. It is necessary to include an estimate of drift velocities to reproduce high yields of dust and low wind velocities.

Key words: hydrodynamics – radiative transfer – methods: numerical – stars: AGB and post-AGB – stars: carbon – stars: mass-loss.

1 INTRODUCTION

Winds of asymptotic giant branch (AGB) stars are believed to be driven by radiation pressure on dust grains, which create an outflow when they in turn drag the gas in the atmosphere along. These winds are relatively slow ($\sim$10 $km\,s^{-1}$), but mass-loss rates can be high ($\sim10^{-5}\,M_{\odot}\,yr^{-1}$) owing to high densities. The type of dust forming in AGB-star atmospheres depends on the chemical composition of the gas: oxygen-rich stars (C/O < 1) form mostly silicate-type grains (but also iron dust can form in significant quantities, see Marini et al. 2019), whilst carbon-rich stars (C/O > 1) form mainly amorphous carbon (amC) grains and smaller amounts of grains of SiC and polycyclic aromatic hydrocarbons (PAHs). The latter type of stars is usually referred to as 'carbon stars' and represents evolved stars with initial masses in the range 1.5–4 $M_{\odot}$ that undergo so-called thermal pulses. That is, after the helium shell runs out of fuel, the star derives its energy from hydrogen burning in a thin shell; eventually, accumulated helium from the hydrogen-burning ignites, causing a helium shell flash. During the thermal pulses, which last a few hundred years, material from the inner regions is mixed into the outer layers. This process is referred to as dredge-up and changes the surface composition of the star; in particular, this is how an oxygen-rich AGB star evolves into a carbon star. The amount of carbon expelled by carbon stars is significant and they may thus play a role in the evolution of carbon (and carbonaceous dust) in the universe, although it cannot be ruled out that massive stars may be equally important (e.g. Gustafsson et al. 1999; Mattsson 2010). The carbon production of carbon stars is important and understanding the wind-formation mechanisms is essential to the full picture.

Radiatively accelerated dust grains exert a drag force on the gas; this drag force depends on how well grains couple to the gas, which in turn depends on the radiation flux, the density and temperature of the gas, as well as the extinction and cross-section of dust grains. In case gas and dust are perfectly coupled, often referred to as complete momentum coupling, the momentum gained by dust grains from the radiation pressure is immediately transferred (or 'shared') with the gas. In this case, gas and dust move at the equilibrium drift velocity. Not only is drift ignored when dust and gas are assumed to move with the same velocity [position coupling (PC)], but also the mass of dust particles.

The full system of radiation hydrodynamics including a description of stellar pulsations and drift using one mean dust velocity is, for the first time, modelled by Sandin & Höfner (2003a, hereafter Paper I), Sandin & Höfner (2003b, hereafter Paper II), and Sandin & Höfner (2004, hereafter Paper III) – these works are summarized with Sandin (2003) – who use grey RT and find that models including drift form more dust in the form of larger grains. The numerical approach of these models is improved with the work presented in Sandin (2008, hereafter Paper IV). See, for example, Paper I (and references therein) for a list of earlier studies of cool star stellar winds

* Dedicated to Agda Sandin.
† E-mail: ChristerSandin@yahoo.se

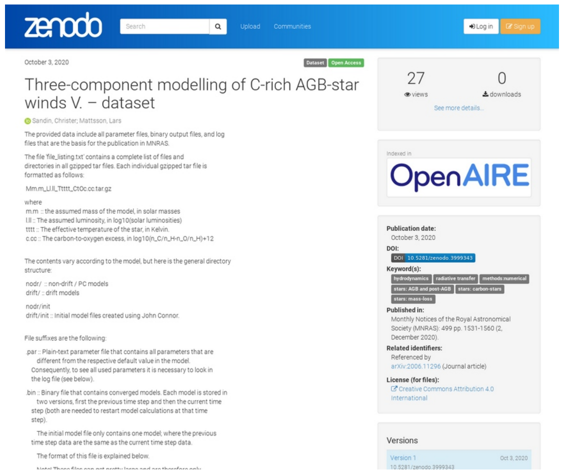

zenodo Search Upload Communities Log in Sign up

October 3, 2020 Dataset Open Access

Three-component modelling of C-rich AGB-star winds V. – dataset

Sandin, Christer; Mattsson, Lars

The provided data include all parameter files, binary output files, and log files that are the basis for the publication in MNRAS.

The file 'file_listing.txt' contains a complete list of files and directories in all gzipped tar files. Each individual gzipped tar file is formatted as follows:

Mm.m_Ll.ll_Ttttt_CtOc.cc.tar.gz

where
m.m :: the assumed mass of the model, in solar masses
l.ll :: The assumed luminosity, in log10(solar luminosities)
tttt :: The effective temperature of the star, in Kelvin.
c.cc :: The carbon-to-oxygen excess, in log10(n_C/n_H-n_O/n_H)+12

The contents vary according to the model, but here is the general directory structure:

nodr/ :: non-drift / PC models
drift/ :: drift models

nodr/init
drift/init :: Initial model files created using John Connor.

File suffixes are the following:

.par :: Plain-text parameter file that contains all parameters that are different from the respective default value in the model. Consequently, to see all used parameters it is necessary to look in the log file (see below).

.bin :: Binary file that contains converged models. Each model is stored in two versions, first the previous time step and then the current time step (both are needed to restart model calculations at that time step).

The initial model file only contains one model; where the previous time step data are the same as the current time step data.

The format of this file is explained below.

27 views 0 downloads
See more details...

Indexed in OpenAIRE

Publication date: October 3, 2020
DOI: DOI 10.5281/zenodo.3999343
Keyword(s): hydrodynamics; radiative transfer; methods:numerical; stars: AGB and post-AGB; stars: carbon-stars; stars: mass-loss
Published in: Monthly Notices of the Royal Astronomical Society (MNRAS): 499 pp. 1531-1560 (2, December 2020).
Related identifiers: Referenced by arXiv:2006.11296 (Journal article)
License (for files): Creative Commons Attribution 4.0 International

Versions
Version 1 Oct 3, 2020
10.5281/zenodo.3999343

Download your own copy, open access!

Data are available as well...to use and check our results!

The paper is available on-line, under an open-access license.

As are about 50GB of the presented data; at Zenodo. You'd have to ask me for access to the remaining 750GB of model data we calculated for this paper.

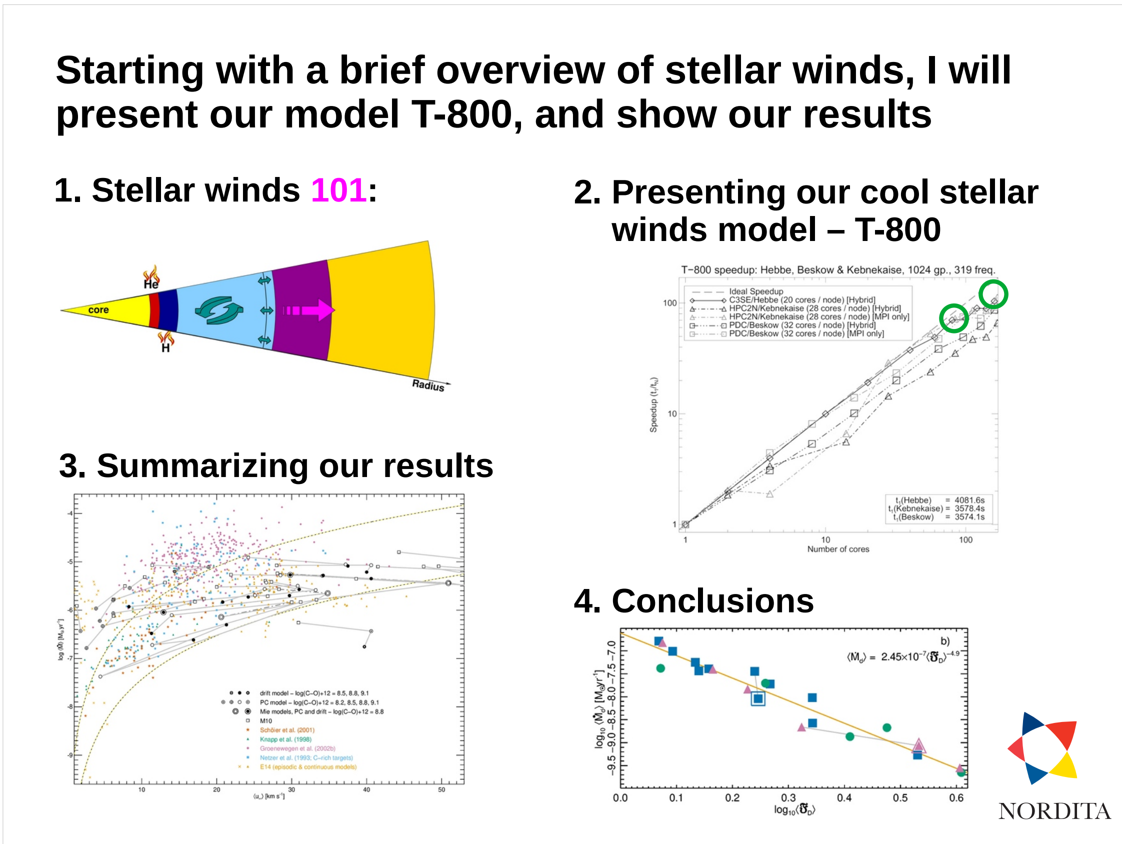

This talk focuses on what our code T-800 can do – and the focus is therefore on simulations

1. I begin with a brief overview of the stellar wind phenomenon, and the kind of physics that is needed to describe it.
2. The physics and numerics that go into the simulations determine what can be done with it
3. I will present some of the results of our study, and our interpretation of the outcome.
4. I finish the talk with conclusions.

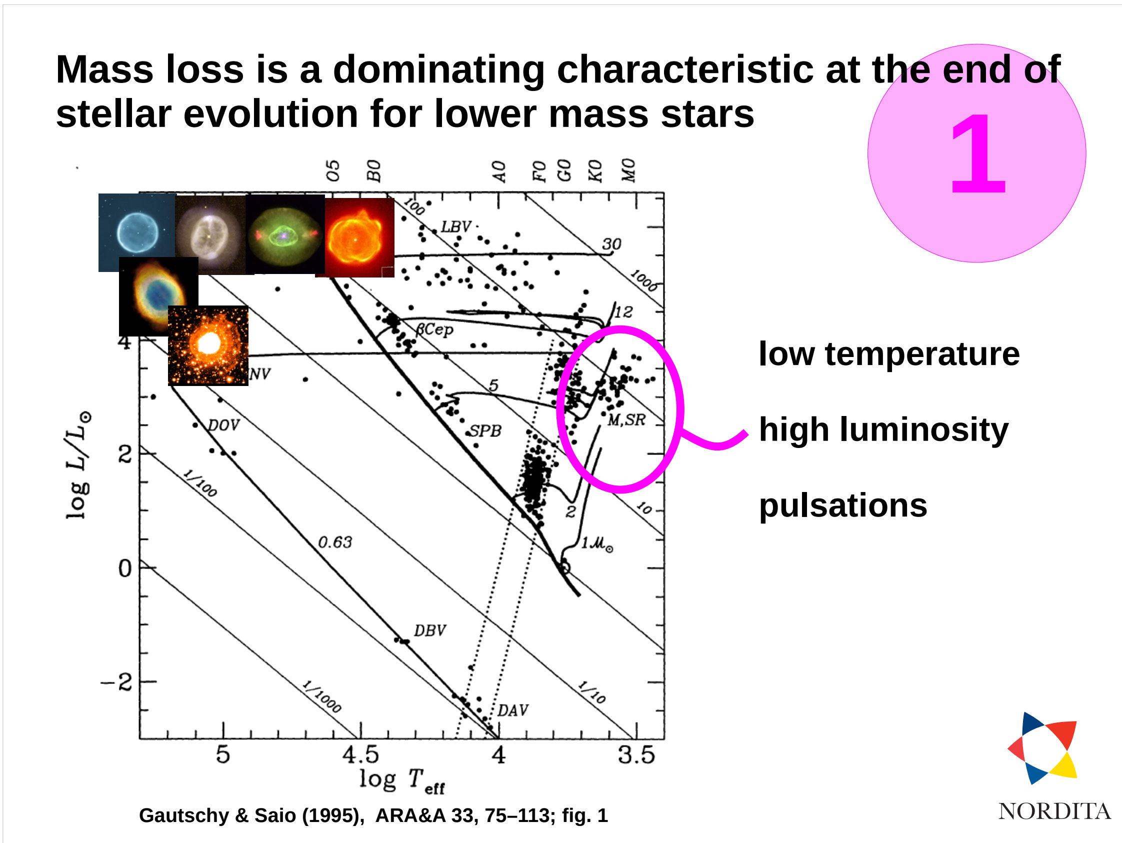

Mass loss, for low to intermediate mass stars dominate on the cool & high luminosity side of the HR-diagram. This is where stars are stripped of their mass, before they become cooling white dwarfs.

The stars, the asymptotic giant stars also pulsate – long period variables – on time scales of hundreds of days.

Since a majority of the stars go through this phase the total amount of mass returned to the ISM of all these stars contributes significantly to the galactic chemical evolution – hence the importance to correctly understand how this mass loss forms.

When the core is exposed, some stars light up as a planetary nebula for a brief moment – the images in the top-left corner show the central parts of some planetary nebulæ.

Note that mass loss if by no means limited to this region, but stars in other parts of the HR-diagram, such as supernovæ, and WR stars also lose mass.

A halo often surrounds the much brighter central parts of the PN – this is the ionized AGB wind

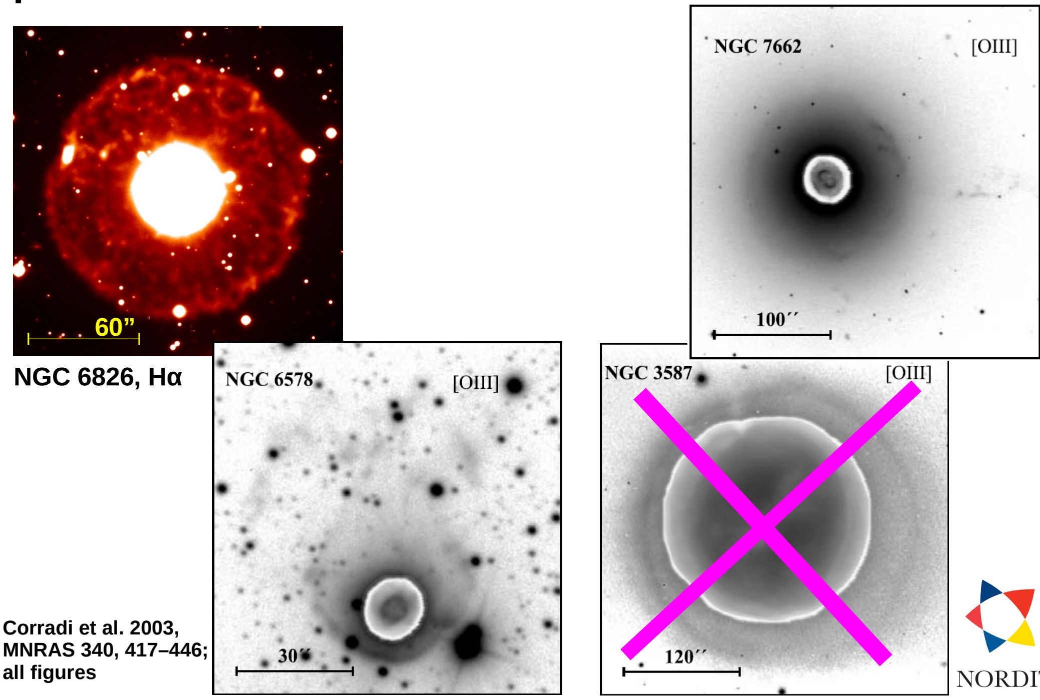

Corradi et al. 2003, MNRAS 340, 417–446; all figures

The figures show halos for four nebulæ of different sizes and ages. The images show the stellar wind of the AGB phase in a faint ionized halo visible at visual wavelengths.

The halo SB is normally a thousand times fainter than in the central PN – this number is different in evolved objects.

In comparison to the central PN proper, the halo has not been restructured by ionization process – physical properties of the halo therefore still contain information about the AGB stellar wind.

For the old owl nebula (lower-right image) the (recombination) halo is very small – this halo also does not contain any information about the AGB wind anymore.

The asymmetric halos in the figures occur due to an interaction with the ISM.

A stellar wind model requires a description of a large part of the AGB star; 3D ...

These stars are three-dimensional – they don’t appear to be all spherically symmetric

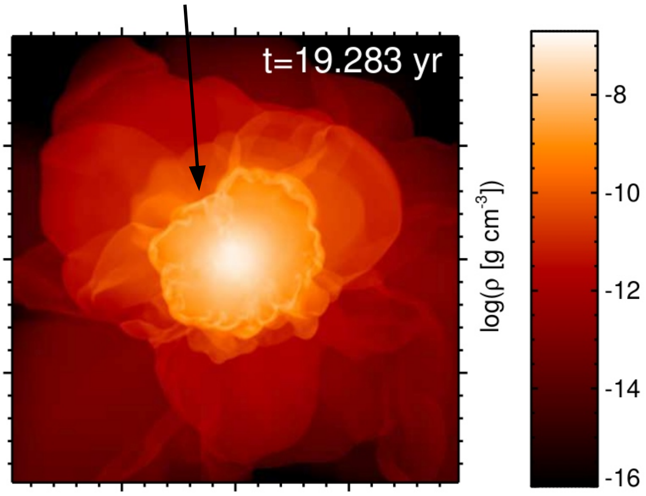

Höfner S. & Freytag B. A&A 2019, 623, A158; fig. 2

NORDITA

Observations have for quite a while indicated that stellar winds are clumpy and asymmetric, i.e. three dimensional.

The image shows the density structure of a three-dimensional wind model that extends out to some 5 R_*, using 401^3 gridpoints.

While this is the ultimate goal – to calculate three dimensional wind models – there are a number of simplifications to the physics that are needed to do this. And the numerical calculations need to be done explicitly...time steps become very small.

A stellar wind model requires a description of a large part of the AGB star; … 1D

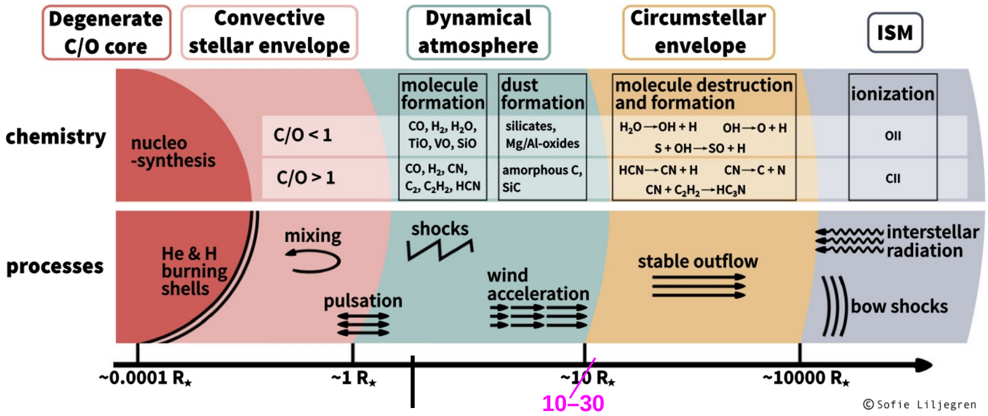

Fig. 1 A schematic figure of an AGB star and its circumstellar environment, including regions and processes of relevance to this review. The stellar radius (R_*) of a typical AGB star is of the order 1 AU (above 100 solar radii). By courtesy of S. Liljegren

Höfner S., Olofsson H. 2018, A&ARv, 26, 1–92

NORDITA

It is, currently, easier to construct a one-dimensional model that contains more physics.

The sketch illustrates the different parts of the star that should be considered in a wind model:

- o a degenerate C/O core
- o He- and H-burning shells
- o a convective stellar envelope – pulsations form (lead to shocks)
- o a dynamical extended atmosphere – simple molecules form
- o a wind acceleration region – where dust forms
- o a circumstellar envelope – where more complex molecules form
- o the surrounding interstellar medium

Most of the mass is in the mantle. A wind model needs to include as much mass as possible of the mantle, and the dynamical atmosphere.

Variation time scales are different in the different parts.

A stellar wind forms in the interaction between the 3(–*N*) components in the extended atmosphere

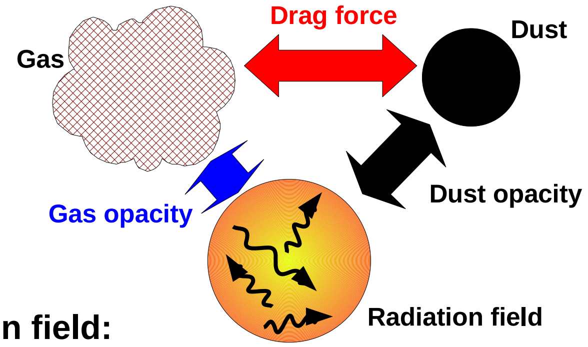

Gas phase:

C-rich (C stars) or
O-rich (M stars) chemistry
..or neither (S stars)

Interaction: gas ↔ radiation field:

Gas opacities: $\kappa_\nu(T_g, \rho_g)$

Interaction: gas ↔ dust component(s):

Drag force: $f_{drag}(u_{gas}, v_{dust}, T_g, \rho_g, \sigma_d)$

NORDITA

Without a driving force, a star does not form a stellar wind, but remains in hydrostatic equilibrium – where thermal pressure is balanced by gravity. A pulsating star, i.e., motions, does not itself give rise to a stellar wind, but may provide suitable conditions for another process to drive a wind.

It is the **interaction** between the components that provides the means to accelerate the bulk of the matter; which is present in the gas component.

The dust component, however, may be very efficient in absorbing radiation. A wind then forms through the **drag force**, which transfers the momentum to the gas.

The direct radiation pressure on the gas, through the gas opacity is NOT enough to drive a wind, but is nevertheless **crucial** to the physical structure of the star.

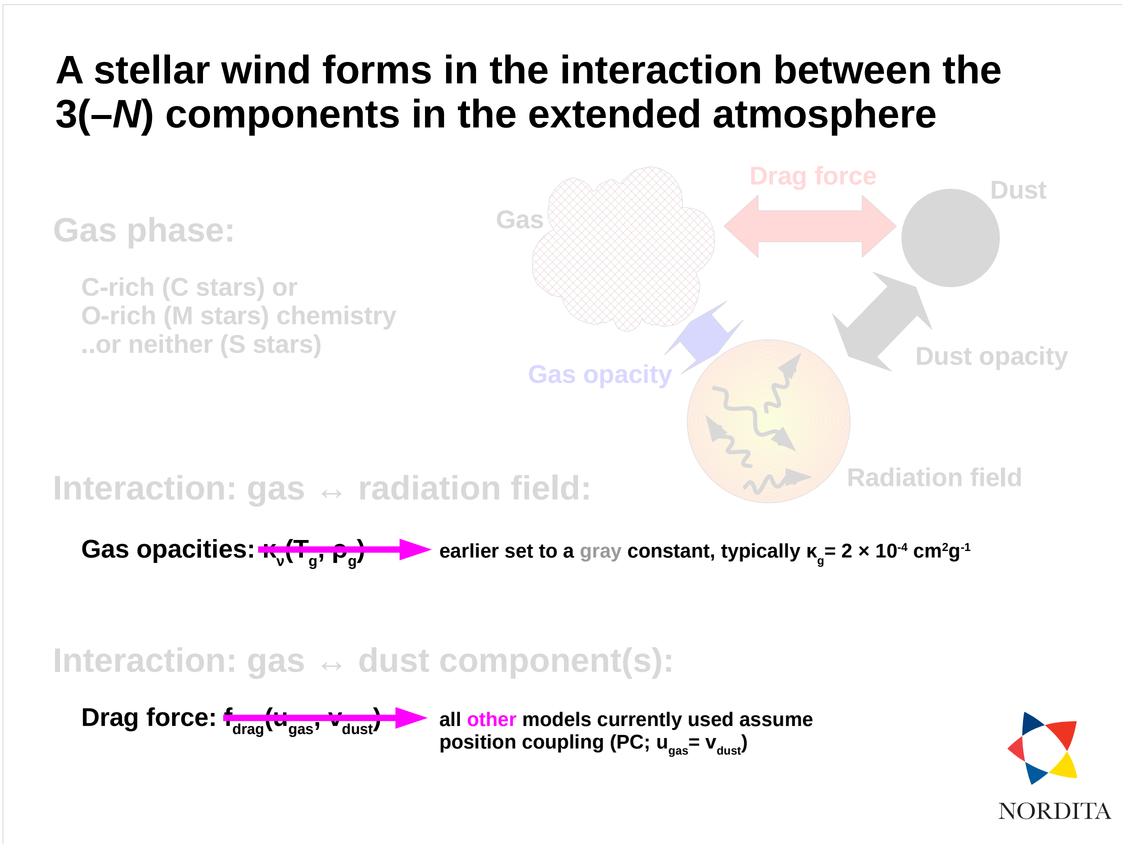

Not all stellar wind models include radiative transfer. Those that do used to set the gas opacity to a constant value (ignoring all level populations), and this results in an awkward density structure (where most of the stellar mass is found in the atmosphere and envelope).

The gas opacity is in fact frequency dependent and depends on vibrational and rotational states of all atoms and molecules in the gas. We interpolate such opacities in temperature and pressure instead of calculating level populations of all atoms and molecules to save time.

Models that do not include the drag force argue that there is position coupling (PC), whereby all momentum attained by the dust is instantaneously transferred to the gas; additionally, the gas and dust move with the same velocity.

Modeling a three-component fluid is challenging. The arguments behind *not* doing it are somewhat vague, and have earlier made kind of sense, probably; because, one has to start somewhere.

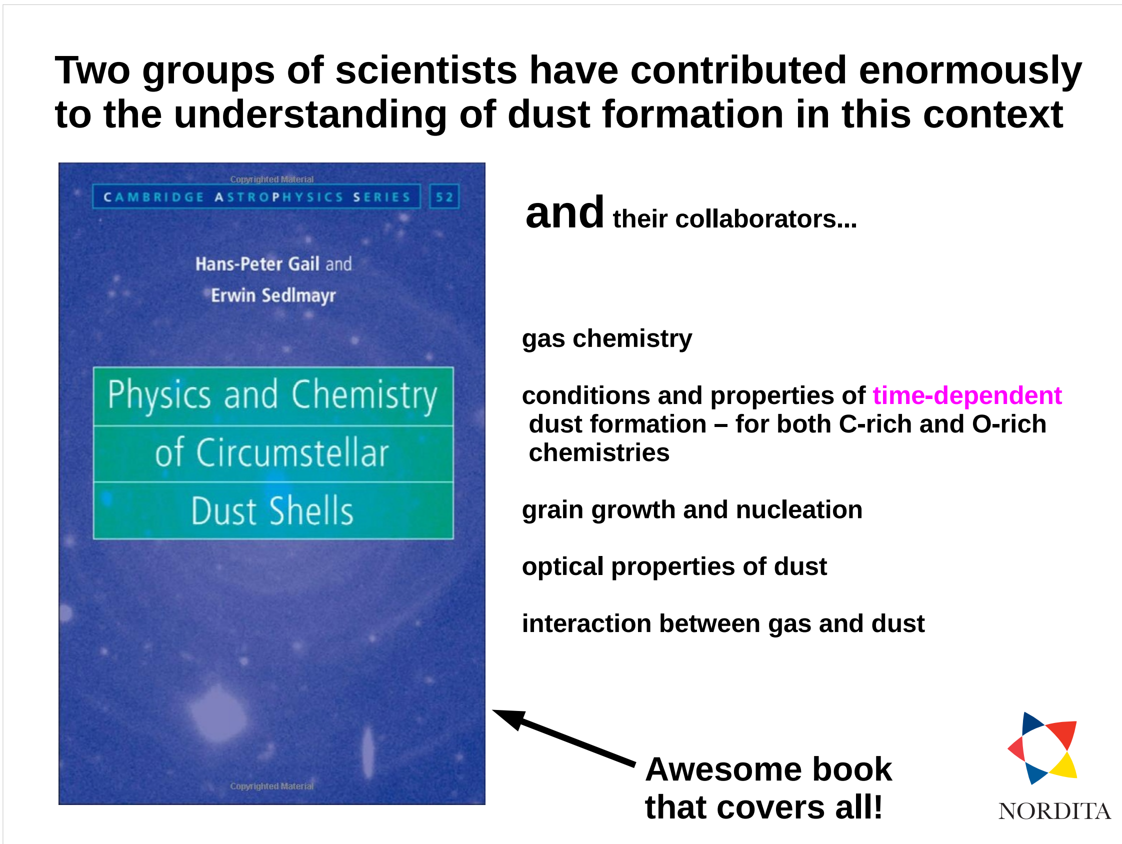

I just want to advertise this awesome book, which contains everything needed to understand the background of the **physics** behind dust-driven stellar winds – for C-rich as well as O-rich chemistries of carbon stars and M stars, respectively.

I personally it is an easier step to begin with this book than plowing through the individual articles of the Sedlmayr's Berlin and Gail's Heidelberg groups.

Present stellar wind models originate in Vienna and are developed in Uppsala – DARWIN (Höfner et al.)

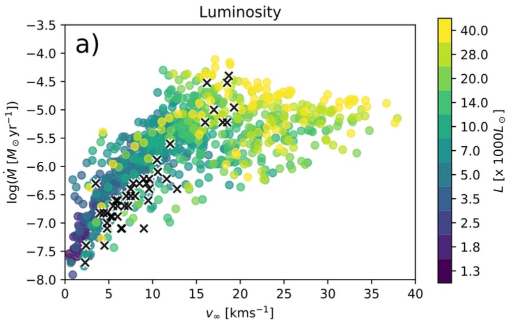

Bladh S., Liljegren S., Höfner S., Aringer B., Marigo P. 2019, A&A, 626, A100; fig. 7 (M stars grid)

Originate with:
Höfner S., Gautschy-Loidl R., Aringer B., Jørgensen U. G. 2003, A&A, 399, 589–601

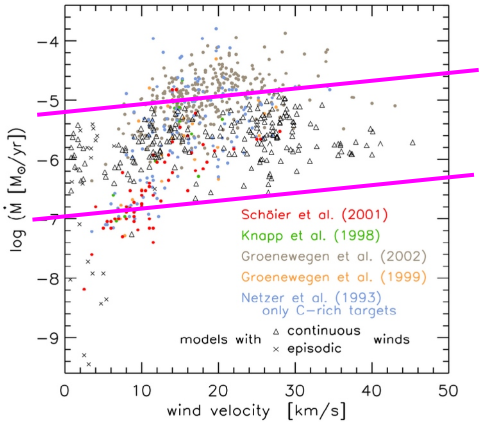

Eriksson K., Nowotny W., Höfner S., Aringer B., Wachter A. 2014, A&A, 566, A95; fig. 4 (C stars grid)

Continued from work of:
Mattsson L., Wahlin R., Höfner S. 2010, A&A, 509, A14

NORDITA

A completely dominating part of current stellar wind models all come from the Uppsala group of Susanne Höfner, who in turn began her work in Vienna.
Both I and Lars began our careers in Uppsala.

The collaborators have extended the original wind models that used C-rich chemistry to include O-rich dust chemistry and have lately been calculating a number of extensive model grids – these grid calculations actually began with Lars's grid study from 2010.

Models and observations overlap – to some extent (in mass loss versus terminal velocity):

+ existing M-star observations show a tight extent, while models span a wider range in velocity.

+ existing C-star observations show a large variation in both mass-loss rate and terminal velocity – where models do not really cover the lowest mass-loss rates at low outflow velocities that well.

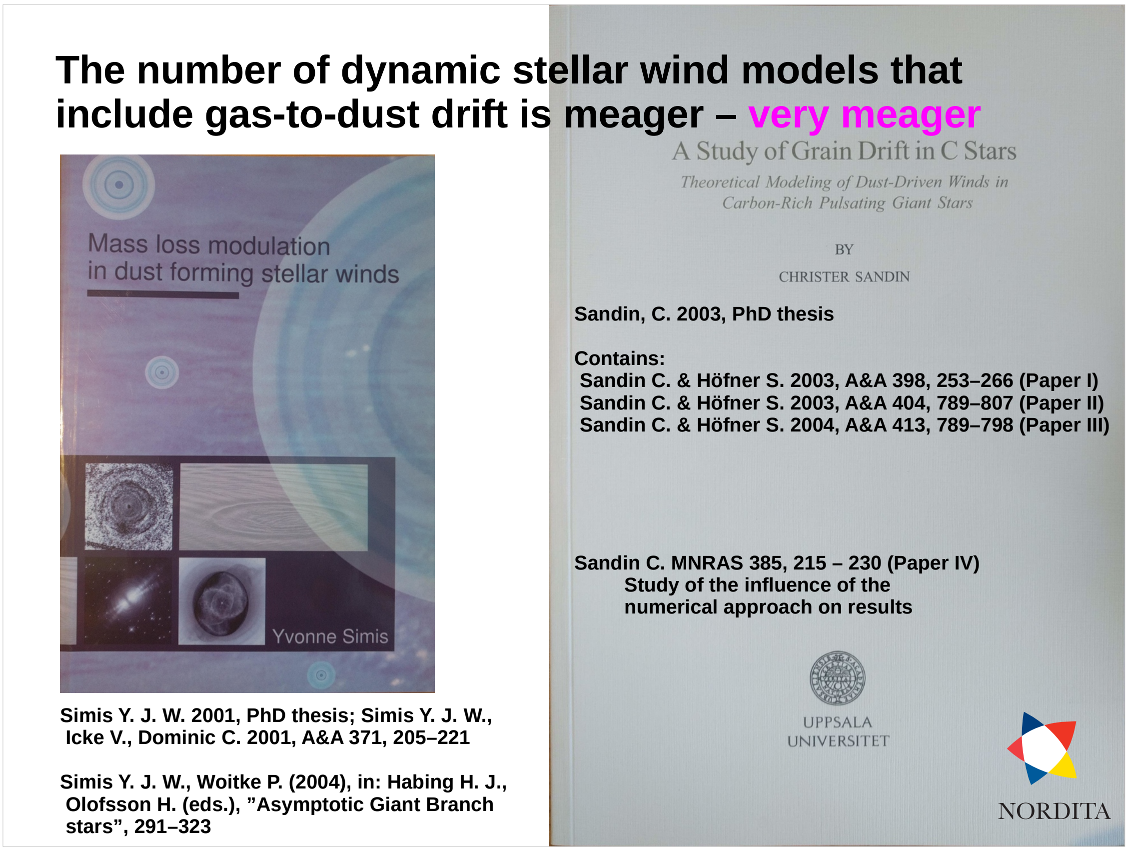

The topic of gas-to-grain drift and stellar winds was pretty popular around the turn of the millenium.

This is no overview, and I only mention two works in this context – both have calculated time-dependent models accounting for drift. (There is a larger number of works that have dealt with stationary wind models.)

Yvonne Simis wrote a wind model all by herself to model long-term variations of mass loss – and she claims to find an explanation to the 100-year separated rings that are observed around PNe.

Her model includes a simplified treatment of radiative transfer, she keeps the inner boundary constant, and presents one model.

My own PhD thesis is based on an earlier model of the Vienna models of S. Höfner; I could write three papers for my thesis, which are all based on gray radiative transport. Later, I wrote a paper on numerical effects in these models.

Nothing much has happened regarding drift since these works.

The number of dynamic stellar wind models that include gas-to-dust drift is meager – very meager

M-type than for C-type AGB stars (cf. Fig. 7). It is worth noting that both C-rich PEDDRO models, for a fixed carbon excess (see Fig. 15, lower panel), and M-type PEDRRO models, for a fixed seed particle abundance (see Fig. 18, bottom panel), can reproduce the observed trends, without including grain drift.[6] A probable explanation is that the time-dependent grain growth process in the PEDDRO models, leading to diverse grain sizes (and grain abundances, in the case of C-rich models), produces a similar self-regulating effect on wind acceleration as grain drift does in SCRA-type models with fixed dust properties (which ignore the time-dependent grain growth pro-

[6] The drift of dust grains relative to the gas by which they are surrounded probably has only modest effects on PEDDRO-type models, since efficient dust formation and radiative acceleration are concentrated to the regions of high gas densities behind the propagating shock waves where drift velocities are low (see, e.g., Sandin and Höfner 2003, 2004). As grain drift introduces a number of extra computational difficulties, it is usually neglected.

Höfner S., Olofsson H. 2018, A&ARv, 26, 1–92; page 59

NORDITA

Drift is currently not considered important at all...the reasoning behind this appear to be based on my work on gray models, where effects were indeed **small**.

There is one saver word in this footnote of the latest AGB wind review paper: the word ”probably”. The text says that drift **probably** only has modest effects on dust-driven wind models. Our new results, as you will see, show that this is not so; drift affects everything.

The number of dynamic stellar wind models that include gas-to-dust drift is meager – very meager

BUT...
BUT...
BUT...

It was never checked what drift does with models using frequency-dependent radiative transfer!

Could it be that drift is important after all?

NORDITA

Because...it has never been checked what the effects of drift are in models using a more realistic density structure – which result when using frequency-dependent radiative transfer.

After having met up with Lars Mattsson about three years ago – which was fully thanks to Beatriz Villaroel we decided to finally start working on this question to find an answer to this conundrum!

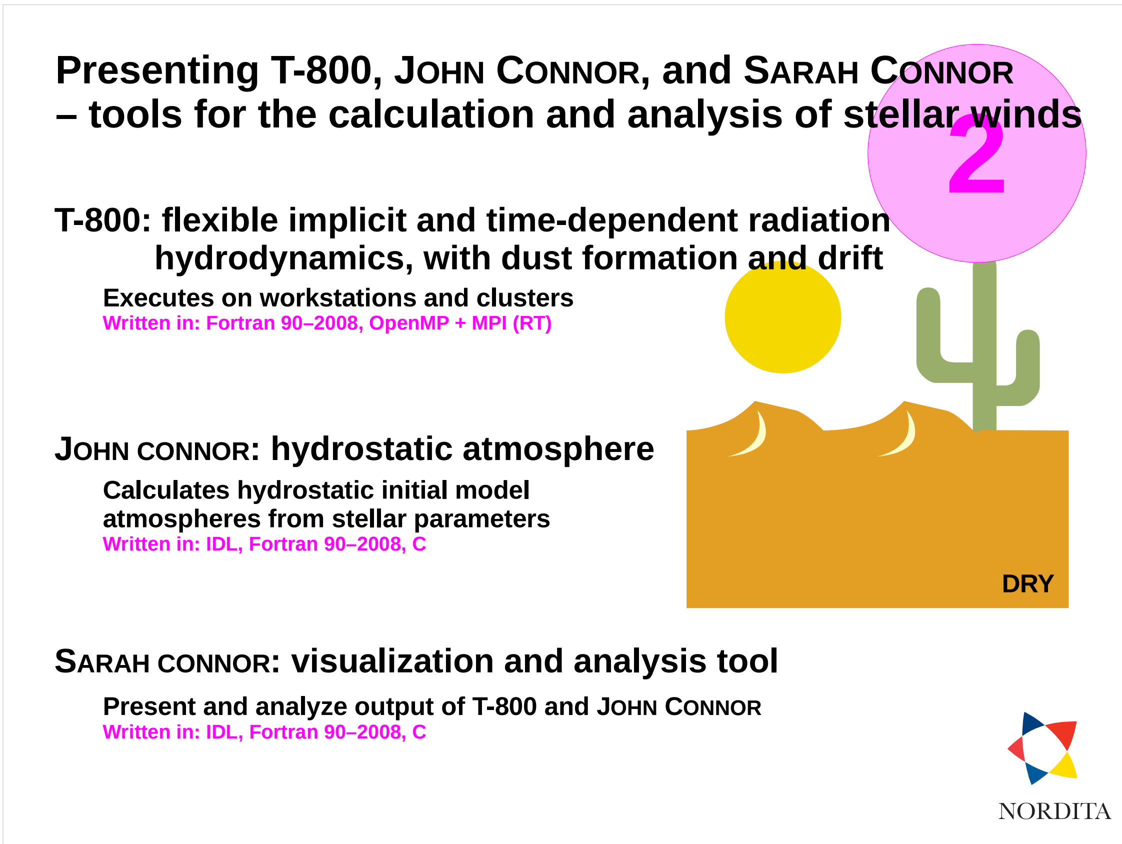

I will now talk about the contents of our model code, T-800.

T-800 is written in Fortran 90–2008:
T-800 includes all physics I ever worked with as well as all kinds of numerical approaches I've attempted.

Everything is configured with, so-called, namelist parameter files. Only a fraction of the nearly 200 provided parameters need to be configured with each run.

Hydrostatic initial models are created using the tool ”John Connor”.
John Connor finds a hydrostatic solution automatically, after setting up the stellar parameters and the radial region of interest.
John Connor provides nearly 100 parameters.

The outcome of both T-800 and John Connor can be analyzed using the visualization and analysis code Sarah Connor, which I wrote as a PhD student to allow me to solve the numerical part of my doctoral studies.

All tools are built around the DRY principle – meaning that there is only one routine that does any particular task – this factor alone reduces the number of bugs.

You might perhaps already have noticed the film ”Terminator 2 – Judgement day” from 1991.

Here, Arnold Schwarzenegger plays a model 101 terminator of the T-800 series of robots. And in this film he’s out to save John Connor, son of Sarah Connor, from being terminated by the T-1000 terminator.

A funny comment on our code names:
The referee notes that we haven’t been 100% consistent in our naming of the code when we compare with the film. Indeed we hadn’t considered all aspects of the spacetime continuum; this was also never the intention.

Assumptions: frequency- and chemistry-dependent gas opacities are key to atmosphere properties

κ(gas), κ(dust), τ^{-1}, drift, RT

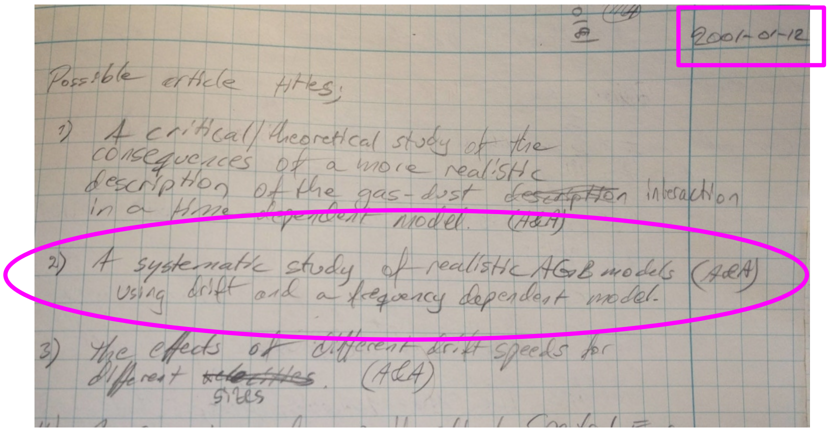

Sandin C., lab journal entry

NORDITA

There are **a lot** of assumptions that go into a model of a dust-driven stellar wind. The assumptions completely determine what the model can do, which is why it is important to know what they are!

One such assumption concerns frequency-dependent gas opacities. It is simply impossible to calculate realistic physical structures without such data.

As you can see in this excerpt of my lab journal, I wanted to do this already before I had hardly begun calculating any models for my PhD thesis (2001-01-12).

And now finally, 20 years later and in collaboration with Lars Mattsson, I am finally able to close the circle and include such data in my models.

Assumptions: frequency- and chemistry-dependent gas opacities are key to atmosphere properties

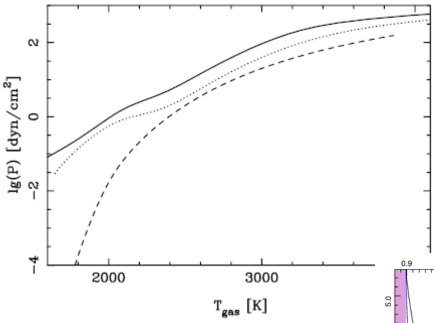

Höfner S. 1999, A&A 346, L9–12; fig. 1

κ(gas), κ(dust), τ^{-1}, drift, RT

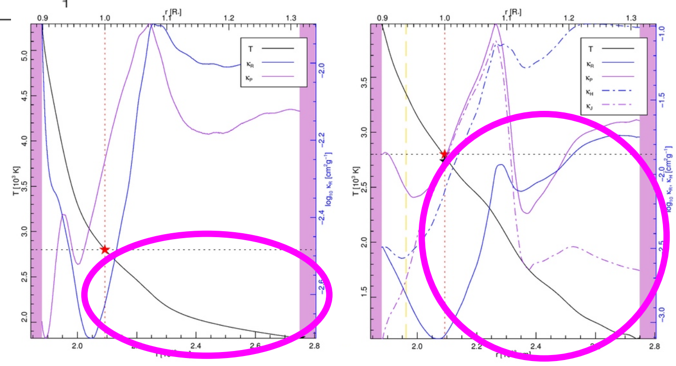

JOHN CONNOR: M=1.0M$_\odot$, L=10$^{3.7}$L$_\odot$, T=2800K, log(C-O)+12=8.80; gray (left panel) and frequency-dependent (right) solutions

NORDITA

Upper left figure – $P_{gas}(T_{gas})$:

A hydrostatic model using 51 frequencies in the radiative transfer is shown with a *solid line*. It agrees pretty well with a MARCS model that is calculated using about 5000 frequencies, *dotted line*.

Compare these two lines with the model that uses gray Planck-mean opacities, *dashed line* – the pressure is simply off by orders of magnitude at low temperatures.

Lower right figure – $T_{gas}(r\ [R_*])$:

The output of JOHN CONNOR illustrates differences in the outer temperature structure between the first gray model and the resulting relaxed frequency-dependent model (319 frequencies).

The outer atmosphere is cooler in the frequency-dependent model.

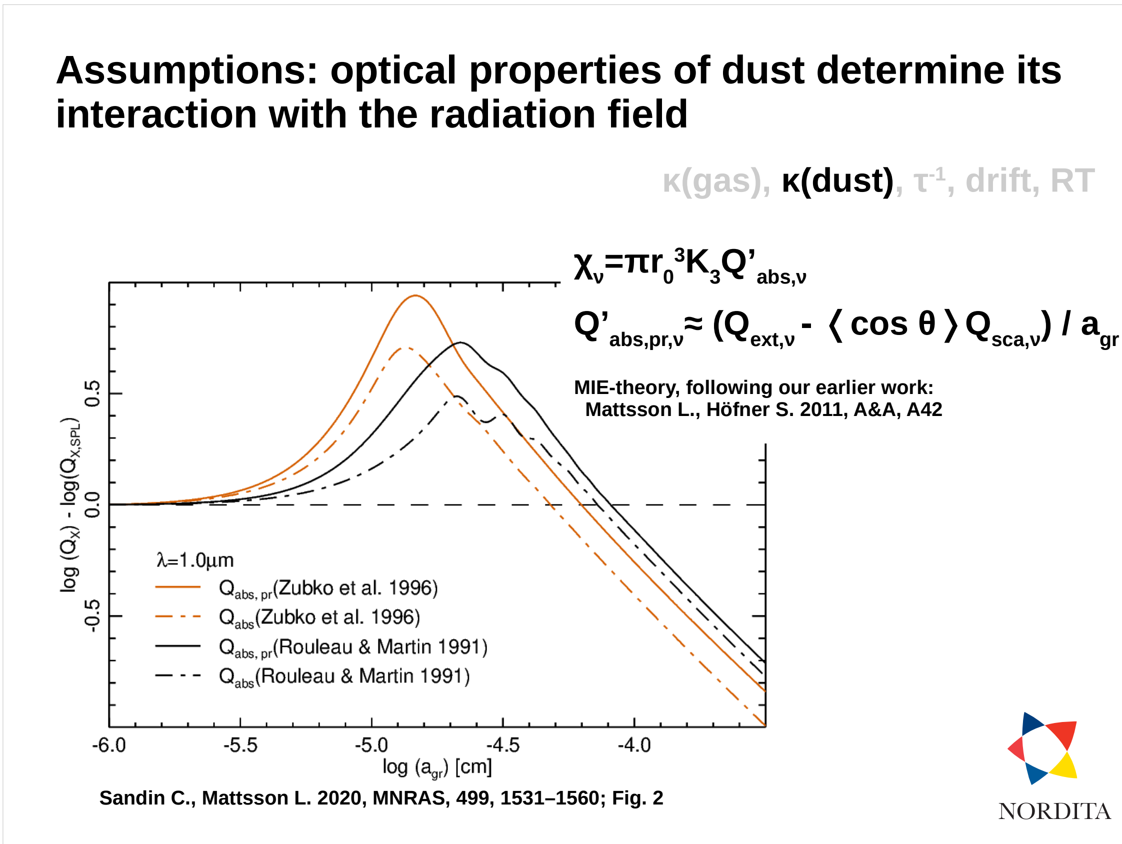

The dust opacity is a function of the material and the wavelength.

As earlier studies do, we make use of the opacity data for amorphous carbon of Rouleau & Martin (*1991*).

The refractive indices are used to calculate the absorption efficiency through the extinction efficiency, the scattering efficiciency, and the scattering angle.

T-800 uses either the small particle limit (SPL) or Mie-theory to calculate the absorption efficiency. In the latter case, we follow our earlier work of Mattsson & Höfner 2011.

The plot illustrates the difference between SPL and Mie-theory absorption efficiencies. At the peak of the curves at some 0.05μm, the difference is about a factor eight. The higher opacity in models using Mie theory could be significant!

Assumptions: dust formation occurs where conditions are right – at low temperatures and high densities

κ(gas), κ(dust), **τ^{-1}**, drift, RT

Carbon-rich dust chemistry:

H, H_2, C, CO, C_2, C_2H, C_2H_2, C_3H, C_3, … → amC

Properties of amorphous carbon:

ρ_{grain} – intrinsic grain density: 1.85 g cm^{-3}
σ_{grain} – grain surface tension: 1400 erg cm^{-2}
α(C) – sticking coefficient: 0.37
α(C_2) – sticking coefficient: 0.34
α(C_2H) – sticking coefficient: 0.34
α(C_2H_2) – sticking coefficient: 0.34

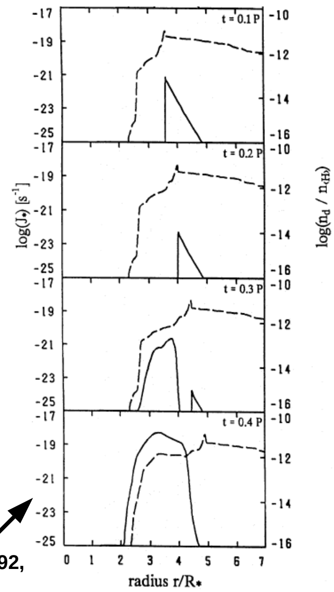

Fleischer A. J., Gauger A., Sedlmayr E. 1992, A&A, 266, 321–339; fig. 5

NORDITA

Dust formation in the form of grain nucleation and grain growth is handled according to the framework of the Berlin group, using moments of the grain size distribution.

At the moment, we're using a carbon-rich chemistry – which forms amorphous carbon.

The gas is assumed to be in chemical equilibrium, which provides number densities of the components that contribute to the formation of amorphous carbon: C, C_2, C_2H, C_2H_2, C_3, and C_3H.

Properties of the dust grains are described with a number of parameters:

+ We use spherical particles.
+ The intrinsic grain density (we use the same value as Rouleau & Martin did with their opacity data)
+ The grain surface tension
+ The sticking coefficient...which fraction of impinging carbon atoms actually stick to the dust grains.

Assumptions: dust formation occurs where conditions are right – at low temperatures and high densities

κ(gas), κ(dust), τ^{-1}, drift, RT

Carbon-rich dust chemistry:

H, H_2, C, CO, C_2, C_2H, C_2H_2, C_3H, C_3, ... → amC

Properties of amorphous carbon:

ρ_{grain} – intrinsic grain density: 1.85 g cm^{-3}
σ_{grain} – grain surface tension: 1400 erg cm^{-2}
α(C) – sticking coefficient: 0.37
α(C_2) – sticking coefficient: 0.34
α(C_2H) – sticking coefficient: 0.34
α(C_2H_2) – sticking coefficient: 0.34

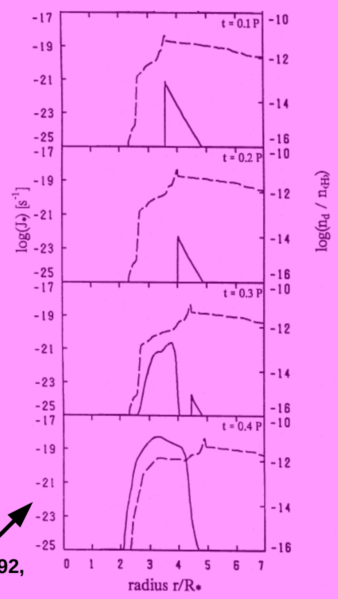

Fleischer A. J., Gauger A., Sedlmayr E. 1992, A&A, 266, 321–339; fig. 5

NORDITA

Other studies of stellar winds on the AGB – including all models calculated using the DARWIN code – have agreed to use the value 1.0 with all atom and molecule coefficients; this is loosely termed the ”Copenhagen agreement”, which also includes other used grain-property values.

We see no reason to not use the originally measured values. It seems more realistic that not all particles that hit a dust grain stick to it.

T-800 can of course use any values one wishes to use with any of these parameters.

Assumptions: dust formation occurs where conditions are right – at low temperatures and high densities

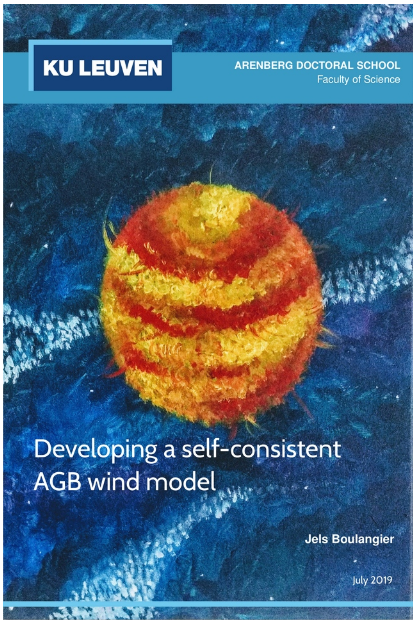

κ(gas), κ(dust), **τ^{-1}**, drift, RT

MPI-ARMVAC + KROME

Presents a much more complete treatment of non-equilibrium nucleation and grain formation

They account for 583 reactions in an O-rich chemistry

Presently, no radiative pressure on grains

Boulangier J. 2019 (Katholieke Universiteit te Leuven)

NORDITA

The dust formation description of the Berlin group and T-800 (and DARWIN) is by no means the final description.

There are recent developments in the field of grain nucleation and grain growth occurring under non-equilibrium conditions. The thesis of Jels Boulangier presents new 3D models that account for all this.

These models are not stellar winds, yet, as there is no radiation pressure on the formed grains.

Assumptions: accelerated dust grains drag gas particles through collisions – microscopic process

κ(gas), κ(dust), τ^{-1}, **drift**, RT

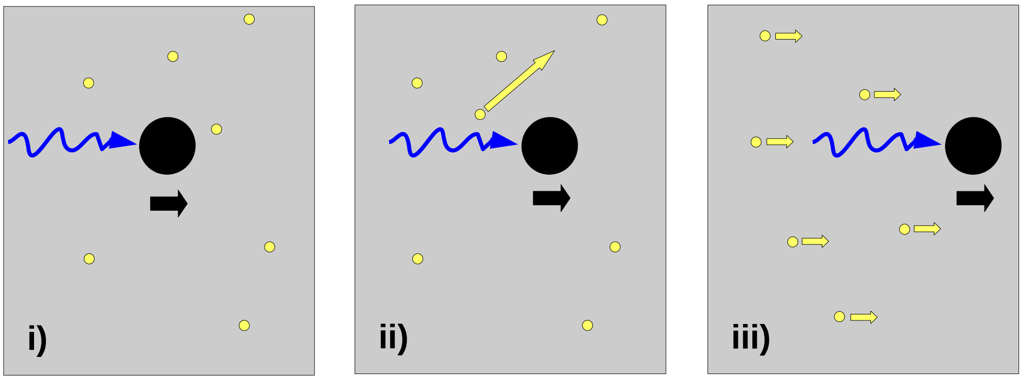

The drag force (f_{drag}) depends on:

- **particle geometry**
- **flow conditions**
- **thermodynamical conditions**
- **type of collisions**

See, for example: Sandin C., Höfner S. 2003, A&A, 398, 253–266

NORDITA

The drag force transfers momentum by collisions with individual particles in the gas – microscopic process. These gas particles then distribute the momentum to the other gas particles. The transfer is mostly assumed to be complete – complete momentum coupling.

Dust grains are in the free molecular flow regime, i.e., there are no collisions between individual dust grains (no coagulation). The results of one collision with a gas particle will also never affect another dust grain.

The drift velocity is non-zero; the number of gas-dust collisions increases with the drift velocity.

The drag force is grain-size dependent – i.e., a stellar wind is really a multi-component fluid.

T-800 currently accounts for one average dust velocity – the model consequently has three components.

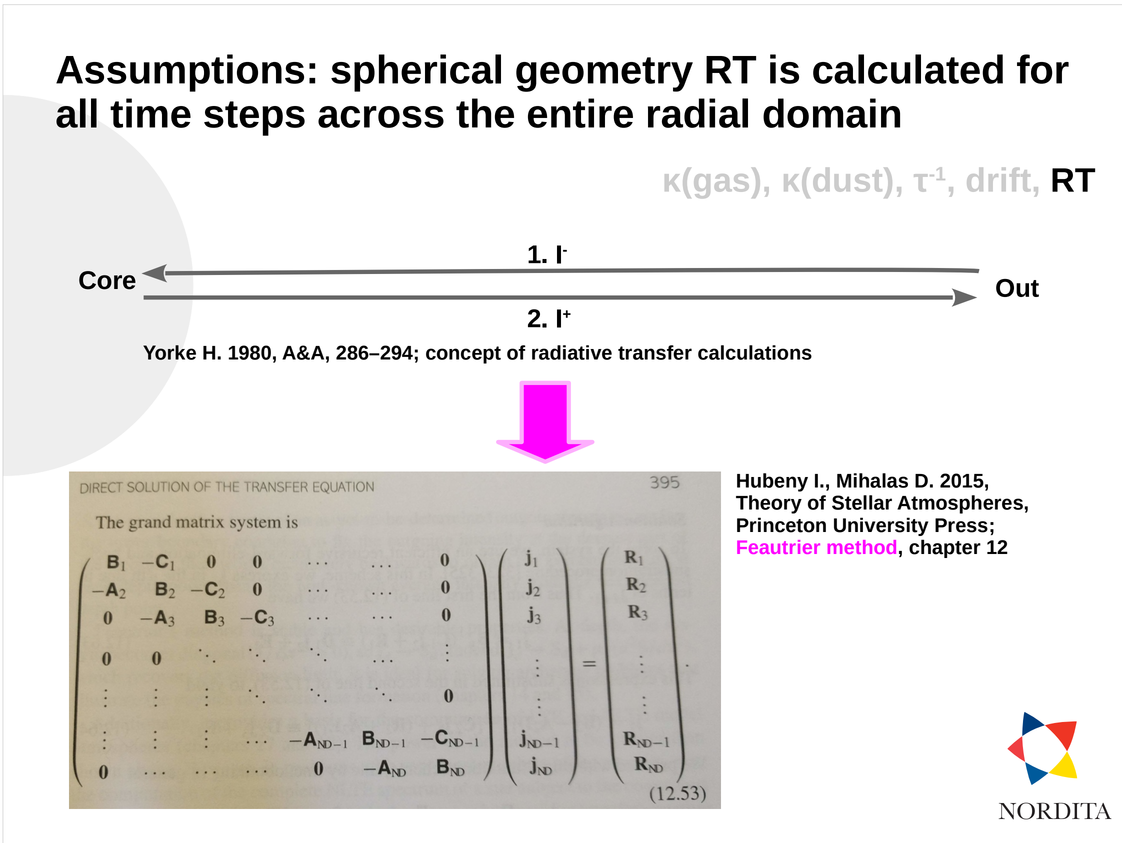

In the radiation hydrodynamic models, the radiation field is described with radiative moments; **J** and **H**.

It is in addition necessary to solve the equation of radiative transfer to close the system of equations.

The radiative transfer equation is solved for **time independently**, separately for each frequency (we use N_ν=319) – this is possible since we do not account for frequency redistribution.

Our earlier models have used the solution approach of Harold Yorke (1980), which sums up the contribution to the radiation field in each cell separately, first moving inwards and then outwards.

We've found this approach to be sometimes unstable and have implemented a solver using the Feautrier method; this approach yields a more stable solution is.

T-800 can, of course, use either one of these two approaches.

Assumptions: time-independent radiative transfer without freq.-redistr., calculated at N(λ) frequencies

κ(gas), κ(dust), τ^{-1}, drift, **RT**

Following the example of Höfner et al. 2003,
T-800 introduces frequency-dependent radiative transfer

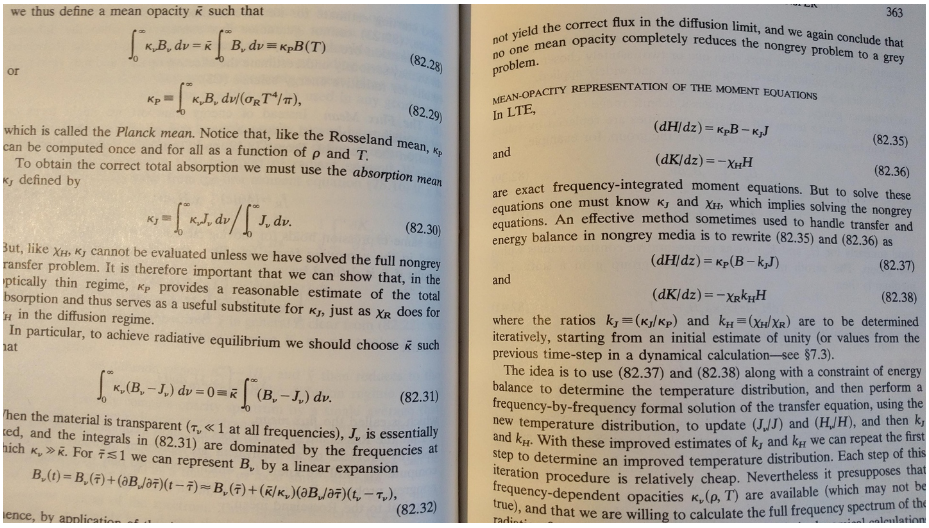

we thus define a mean opacity $\bar{\kappa}$ such that

$$\int_0^\infty \kappa_\nu B_\nu \, d\nu = \bar{\kappa} \int_0^\infty B_\nu \, d\nu \equiv \kappa_P B(T) \quad (82.28)$$

or

$$\kappa_P \equiv \int_0^\infty \kappa_\nu B_\nu \, d\nu / (\sigma_R T^4/\pi), \quad (82.29)$$

which is called the *Planck mean.* Notice that, like the Rosseland mean, κ_P can be computed once and for all as a function of ρ and T.

To obtain the correct total absorption we must use the *absorption mean* κ_J defined by

$$\kappa_J \equiv \int_0^\infty \kappa_\nu J_\nu \, d\nu \Big/ \int_0^\infty J_\nu \, d\nu. \quad (82.30)$$

But, like χ_H, κ_J cannot be evaluated unless we have solved the full nongrey transfer problem. It is therefore important that we can show that, in the optically thin regime, κ_P provides a reasonable estimate of the total absorption and thus serves as a useful substitute for κ_J, just as χ_R does for χ_H in the diffusion regime.

In particular, to achieve radiative equilibrium we should choose $\bar{\kappa}$ such that

$$\int_0^\infty \kappa_\nu (B_\nu - J_\nu) \, d\nu = 0 \equiv \bar{\kappa} \int_0^\infty (B_\nu - J_\nu) \, d\nu. \quad (82.31)$$

When the material is transparent ($\tau_\nu \ll 1$ at all frequencies), J_ν is essentially fixed, and the integrals in (82.31) are dominated by the frequencies at which $\kappa_\nu \gg \bar{\kappa}$. For $\bar{\tau} \lesssim 1$ we can represent B_ν by a linear expansion

$$B_\nu(t) = B_\nu(\bar{\tau}) + (\partial B_\nu/\partial \bar{\tau})(t - \bar{\tau}) \approx B_\nu(\bar{\tau}) + (\bar{\kappa}/\kappa_\nu)(\partial B_\nu/\partial \bar{\tau})(t_\nu - \tau_\nu), \quad (82.32)$$

Hence, by application ...

363

not yield the correct flux in the diffusion limit, and we again conclude that no one mean opacity completely reduces the nongrey problem to a grey problem.

MEAN-OPACITY REPRESENTATION OF THE MOMENT EQUATIONS

In LTE,

$$(dH/dz) = \kappa_P B - \kappa_J J \quad (82.35)$$

and

$$(dK/dz) = -\chi_H H \quad (82.36)$$

are exact frequency-integrated moment equations. But to solve these equations one must know κ_J and χ_H, which implies solving the nongrey equations. An effective method sometimes used to handle transfer and energy balance in nongrey media is to rewrite (82.35) and (82.36) as

$$(dH/dz) = \kappa_P (B - k_J J) \quad (82.37)$$

and

$$(dK/dz) = -\chi_R k_H H \quad (82.38)$$

where the ratios $k_J \equiv (\kappa_J/\kappa_P)$ and $k_H \equiv (\chi_H/\chi_R)$ are to be determined iteratively, starting from an initial estimate of unity (or values from the previous time-step in a dynamical calculation—see §7.3).

The idea is to use (82.37) and (82.38) along with a constraint of energy balance to determine the temperature distribution, and then perform a frequency-by-frequency formal solution of the transfer equation, using the new temperature distribution, to update (J_ν/J) and (H_ν/H), and then k_J and k_H. With these improved estimates of k_J and k_H we can repeat the first step to determine an improved temperature distribution. Each step of this iteration procedure is relatively cheap. Nevertheless it presupposes that frequency-dependent opacities $\kappa_\nu(\rho, T)$ are available (which may not be true), and that we are willing to calculate the full frequency spectrum of the ...

Mihalas D., Weibel-Mihalas B. 1984, "Foundations of Radiation Hydrodynamics"; §82

NORDITA

Mihalas and Weibel-Mihalas (1984) present a method to handle the frequency-dependent radiative transfer – we follow their approach fully.

The frequency-dependent gas and dust opacities are weighted with the radiative moments that result from the radiative-transfer calculations. Out comes the weighted opacities κ_H, κ_J, and κ_S, as well as the dust temperature T_d and these properties are used in the radiation hydrodynamic equations.

Numerical considerations: number of gridpoints; implicit solution; use adaptive grid equation, or not

Radiative transfer + drift = stiff system of equations → **Implicit solution**

Sandin C. 2008, MNRAS, 385, 215–230; fig. 1, using N_{grid} = 500

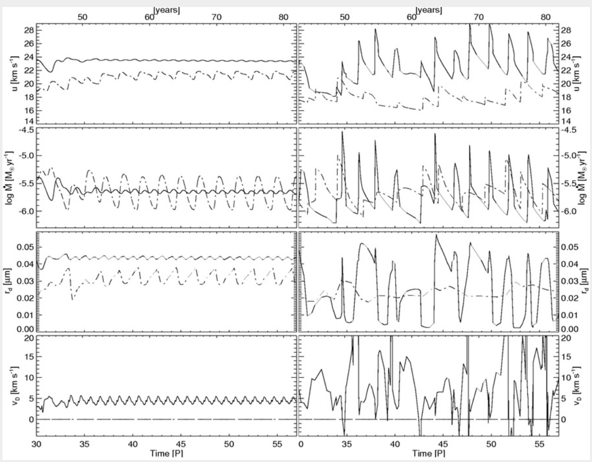

We find irregular structures using the adaptive-grid equation

→

we do not use the adaptive-grid equation to resolve shocks

Here, we compensate by using a high spatial resolution with N_{grid} = 1024

(Compare: DARWIN models use N_{grid} = 100)

NORDITA

It is impossible to calculate radiation hydrodynamics without considering the numerical approach.

T-800 calculates both radiative transfer and drift – both these components make the system of equations stiff, i.e. time steps must be very short unless an implicit solution is used.

I present a study of numerical accuracy with Sandin (2008).
Where I advocate avoiding resolving shocks using the adaptive grid equation.
Because, the grid equation introduces irregular structures that are not there without the grid.
Advocates of the grid equation argue that the grid equation **must be used** to resolve shocks!

I disagree – more shocks are modeled accurately when the grid equation is not used.

We compromise by using 1024 gridpoints in our models; models of the DARWIN code use 100 gridpoints.

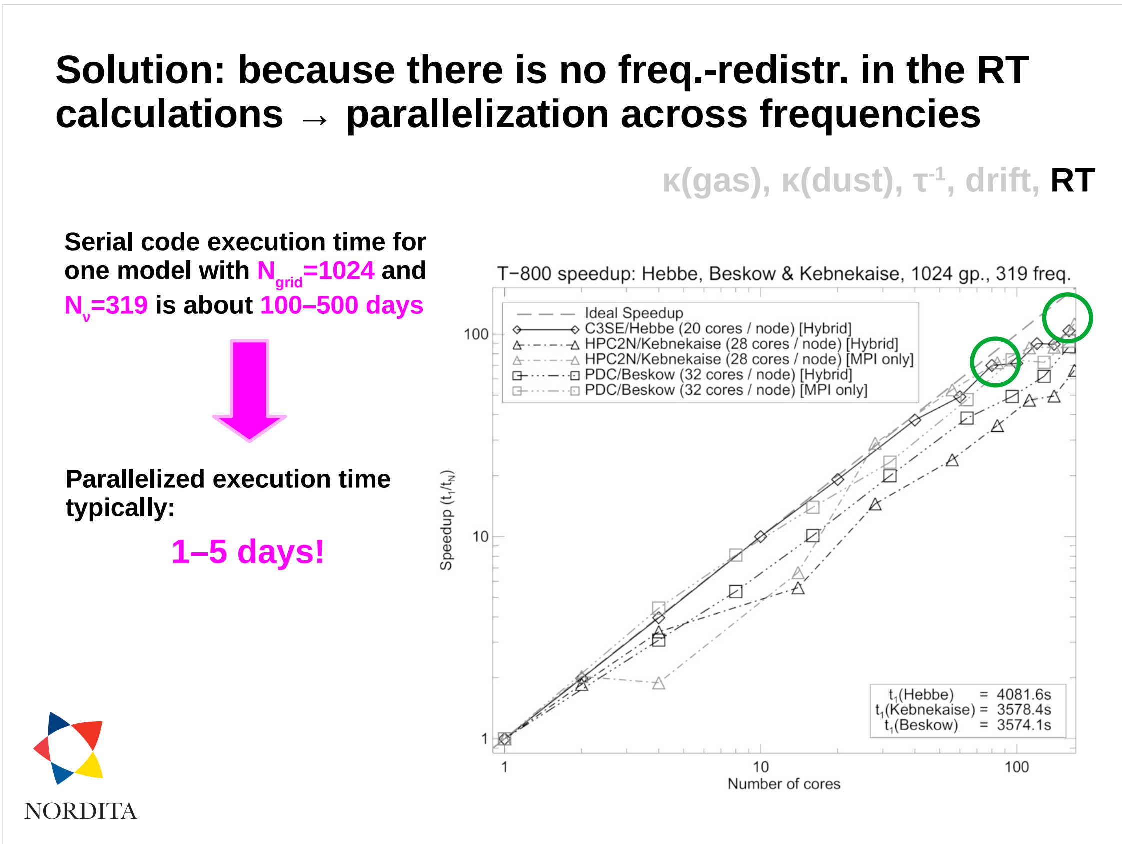

Calculation times become enormous with the number of frequencies and gridpoints we use, in particular considering that T-800 is a one-dimensional code.
Each model requires some 100–500 days of core time to finish.

Because the radiative transfer is calculated for each frequency separately, the approach is highly parallelizable. T-800 makes good use of this fact.

Radiative transfer calculations are split between multiple cores using either OpenMP or MPI, or both (hybrid).

The speedup plot reveals a speedup of about 110 using 160 cores, which implies that each core handles two frequencies.

Running on a cluster using 160 cores, it takes some 1 to 5 days to calculate a model; this is actually feasible!

Results depend on the period-luminosity relation that is used with all these models to simulate pulsations

κ(gas), κ(dust), τ^{-1}, drift, **RT**

Hmm...seemingly an inconsistency!

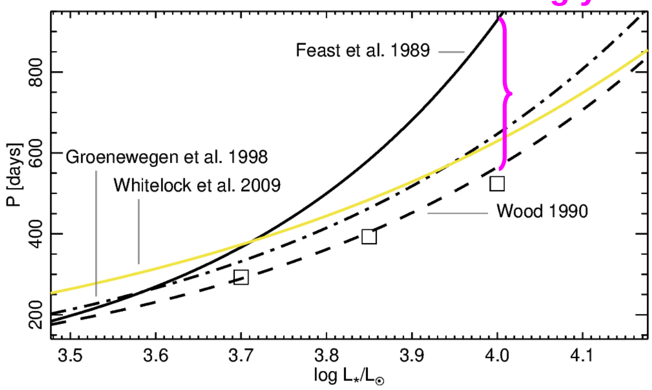

Sandin C., Mattsson L. 2020, MNRAS, 499, 1531–1560; Fig. 1

NORDITA

Stellar pulsations are modelled by varying the inner boundary radially with a sinusoidal function.

We use the same relation as in all our earlier papers on C star winds.

Our pulsation periods are shorter than observations predict. Earlier studies have shown that this can lead to differences...this is important to keep in mind when evaluating the models.

The radial structure of two PC model setups where N_{grid}=100 and 1024

3

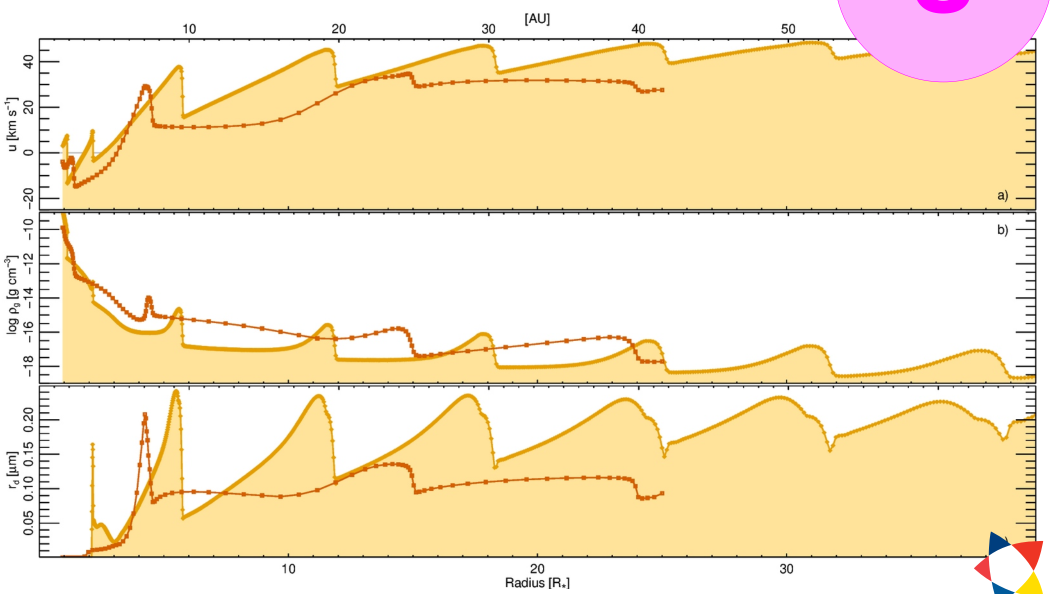

Sandin C., Mattsson L. 2020, MNRAS, 499, 1531–1560; Fig. 7

NORDITA

Here I show two PC models that are calculated using N_{grid}=100 (red line) and N_{grid}=1024 (orange filled line).

The red line extends out to 25 stellar radii (R*), which is how we fathom that DARWIN models are calculated. We calculate our own models out to 40R* to include as much as possible of the wind formation region.

Explain: from the top, the plots show the gas velocity, gas density, and mean grain radius.

The red line shows a couple of shocks that are reasonably resolved and the structure is also kind of irregular. Note that regions between the shocks are not as well resolved (each diamond symbol is a gridpoint).

The orange line shows a larger number of shocks where all shocks and regions between the shocks are resolved.

Results: comparison between radial structures of a periodic PC model and a more variable drift model

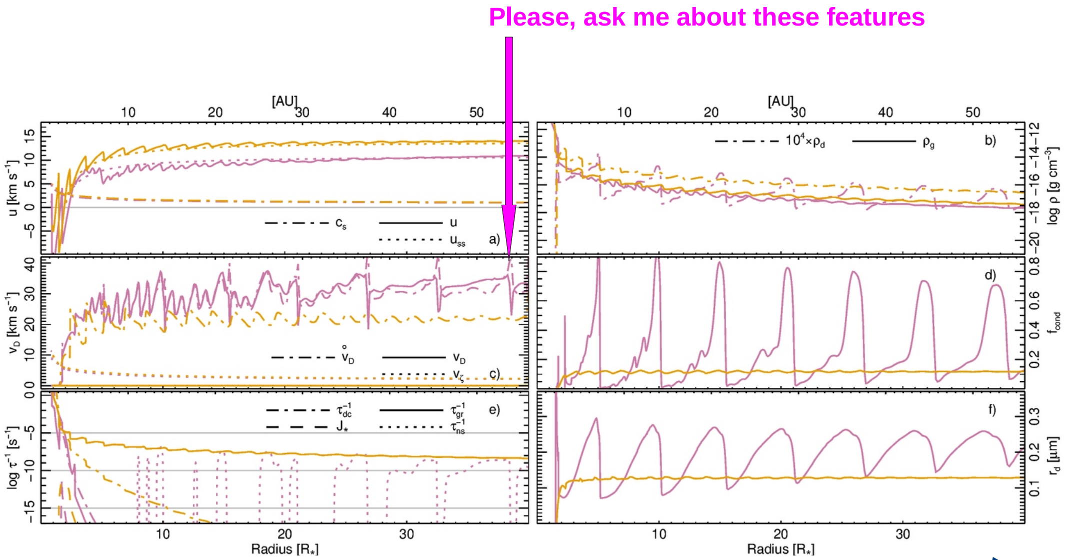

Sandin C., Mattsson L. 2020, MNRAS, 499, 1531–1560; Fig. 8

NORDITA

Here, I show more radial plots of a typical model for a set of properties that are calculated in the models. Each radial plot is a snapshot of the dynamical model at some illustrative point in time. Shocks move from the left to the right.

The plot shows a position-coupled (PC) model [orange lines] and a drift model [purple lines] – both use N_{grid}=1024 and the outer boundary is at $40R_*$. From the top left, the panels show (solid lines) the gas velocity, gas density, drift velocity, degree of condensation, net grain growth, and mean grain radius.

Both models are periodic, and repeat with each pulsation period.

In the drift model, the dust is distributed in distinct shells, with little dust between the shells.

The drift velocity is some 20 km/s in the innermost regions and increases to some 35 km/s in the outer region – these are much higher values than could be attained in my earlier work that use gray Planck-mean models !

Results: comparison between temporally averaged structures of a PC model and a drift model

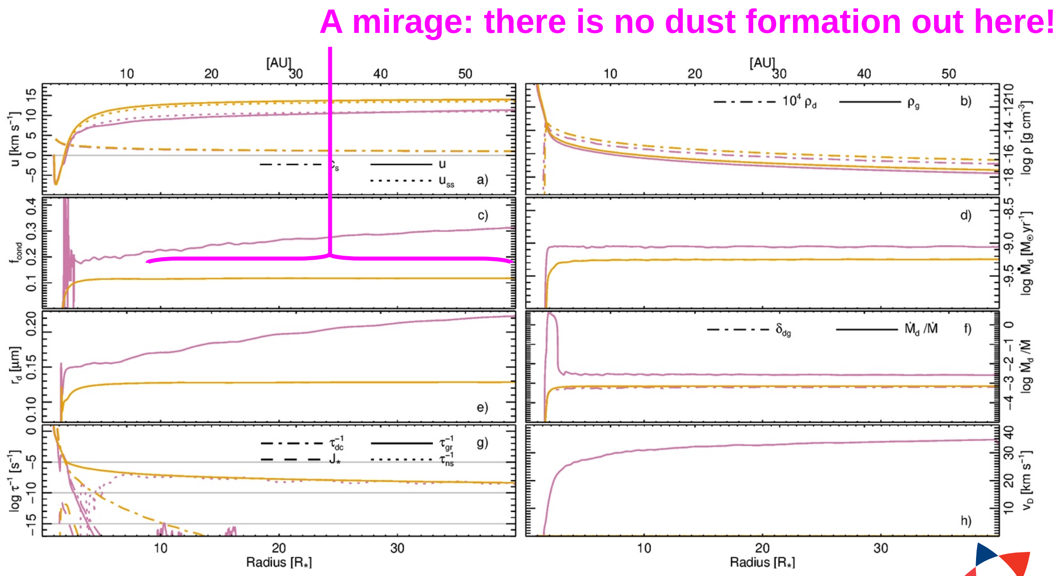

Sandin C., Mattsson L. 2020, MNRAS, 499, 1531–1560; Fig. 9

NORDITA

Observations of stellar winds do not resolve the inner region as well as models do and it makes sense to calculate temporally averaged plots using a couple of pulsation periods.

This plot shows such temporally averaged properties. The panels are shuffled.

However, note that all properties show a fairly smooth variation, reminding more of a stationary structure than irregular time-dependent solutions.

In particular, checking the degree of condensation (panel c) and the mean grain radius (panel e), one could think that there is grain formation in the outer envelope. **However**, this is an illusion: the increasing slope appears when dust in the initially distinct shells leaks into the region between the shells while moving outwards.

Results: comparison between temporal structures of a periodic PC model and a more variable drift model

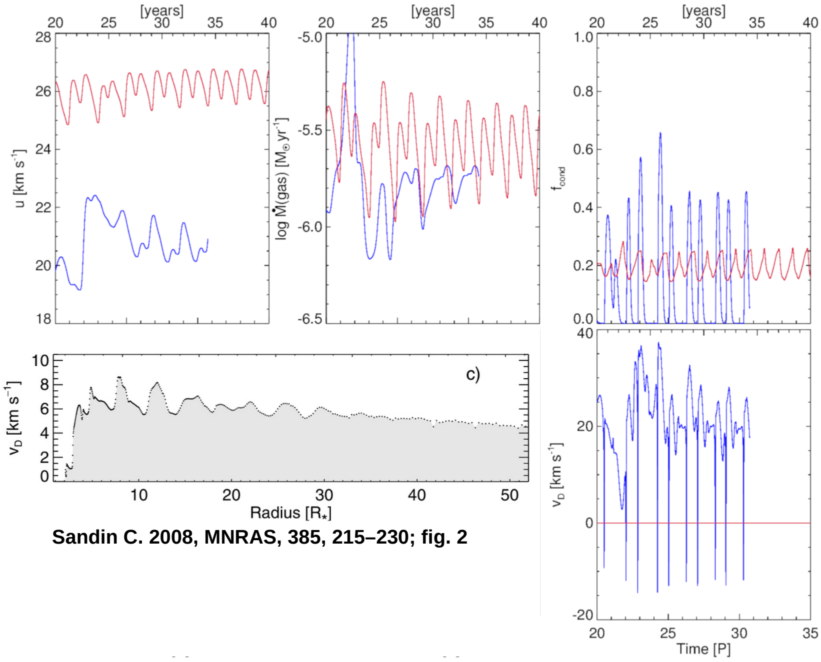

Sandin C. 2008, MNRAS, 385, 215–230; fig. 2

NORDITA

Sampling model values at the outer boundary, one can create a temporal plot of the model structure. And if one then takes the average of these plots, for a suitable range in time, one calculates mean values that can be compared with observations.

With the four panels showing red (PC model) and blue (drift model) lines, we illustrate that most of the new models are actually periodic once they have relaxed, or at least quasi periodic (less stringent than perfectly periodic).

The four panels show the gas velocity, mass loss rate, degree of condensation, and the drift velocity (the troughs in this panel are the same as indicated with the pink arrow in the plot two slides ago).

Compare the new plot of the temporal variation of the drift velocity with a plot of a gray model (lower left panel, right-hand side)– drift velocities are now significantly higher, ~20km/s instead of 4.5km/s.

Temporal plots of DARWIN are also said to be periodic (this is for another set of model parameters)

classification: *wp* – periodic variations in the wind properties

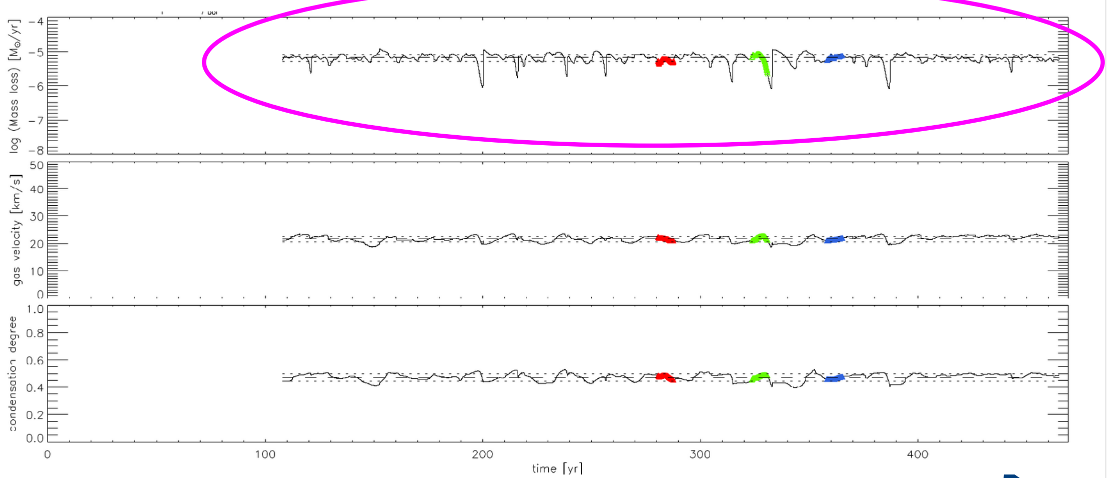

Eriksson K., Nowotny W., Höfner S., Aringer B., Wachter A. 2014, A&A, 566, A95; part of fig. C1, for a model where: T_{eff} = 2600 K, L = $10^{4.0}$ $L_{\odot}$, M = 1.5 $M_{\odot}$, log(C-O)+12 = 8.50, Δu_p = 6 km/s

NORDITA

Eriksson et al. (2014) present one fact sheet per model in their grid study of carbon-rich stars – such fact sheets are available at the CDS for all models [I can only find this fact sheet].

Among other information, the sheet presents temporal plots.

The presented model is said to show periodic variations.

I would personally classify this as an irregular model – compare with our structures on the previous page.

I would say that the variations in our model are **more** periodic.

It seems results are different when Mie-theory is used instead of the SPL with the dust opacity

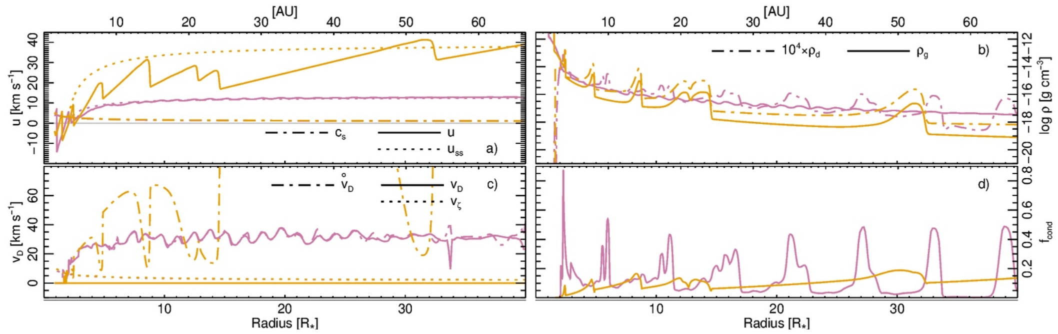

Sandin C., Mattsson L. 2020, MNRAS, 499, 1531–1560; Fig. 13

NORDITA

We calculated three models anew using using Mie-theory instead of the small-particle limit (SPL) for the dust opacity.

In comparison to Mattsson & Höfner 2011, we find that the outflow changes significantly in all models! And in particular in the PC models.

The PC model has not relaxed fully yet – note the peak in the outflow velocity at large radii (top left panel, orange line).

The outflow velocity of the drift model is lower, and shows less variation (i.e. more stationary). The velocity structure seems more periodic.

The amount of formed dust appears to decrease, but simultaneously the drift velocity increases, by some 50-100%; this implies that the flux of grains is about the same as when using the SPL instead).

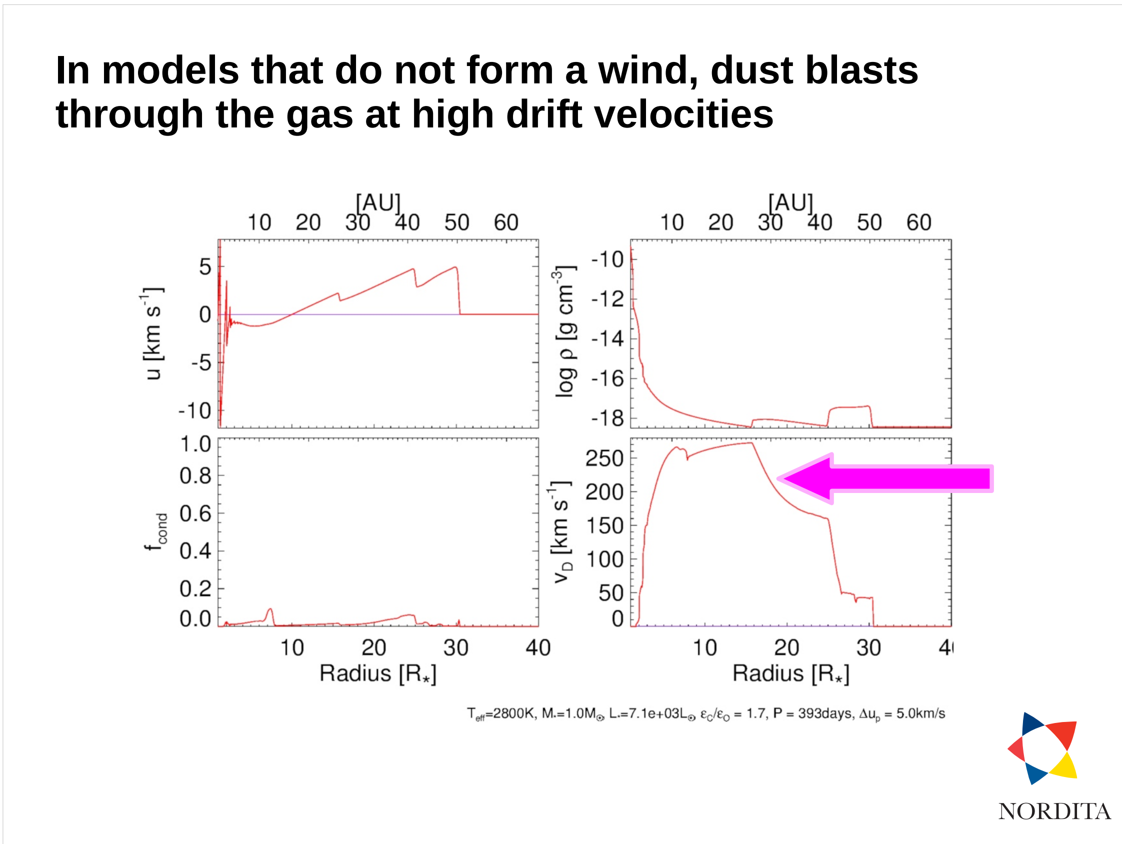

Not all stellar parameters result in a stellar wind.

Here, an attempt is made at forming a wind using drift and such ”non-wind-forming” parameters.

While the outer extent of the ”wind” has here reached about $30R_*$ (see the top left panel), the model has difficulties sustaining an outwards movement of mass.

The degree of condensation is low (lower left panel) – diluted by the high dust velocity (lower right panel), which achieves high values already near the stellar photosphere.

Instead of staying near the star and accumulating – the dust immediately blasts outwards through the gas at high speed.

We find it difficult to form any wind using drift where the corresponding PC model has a low outflow velocity.

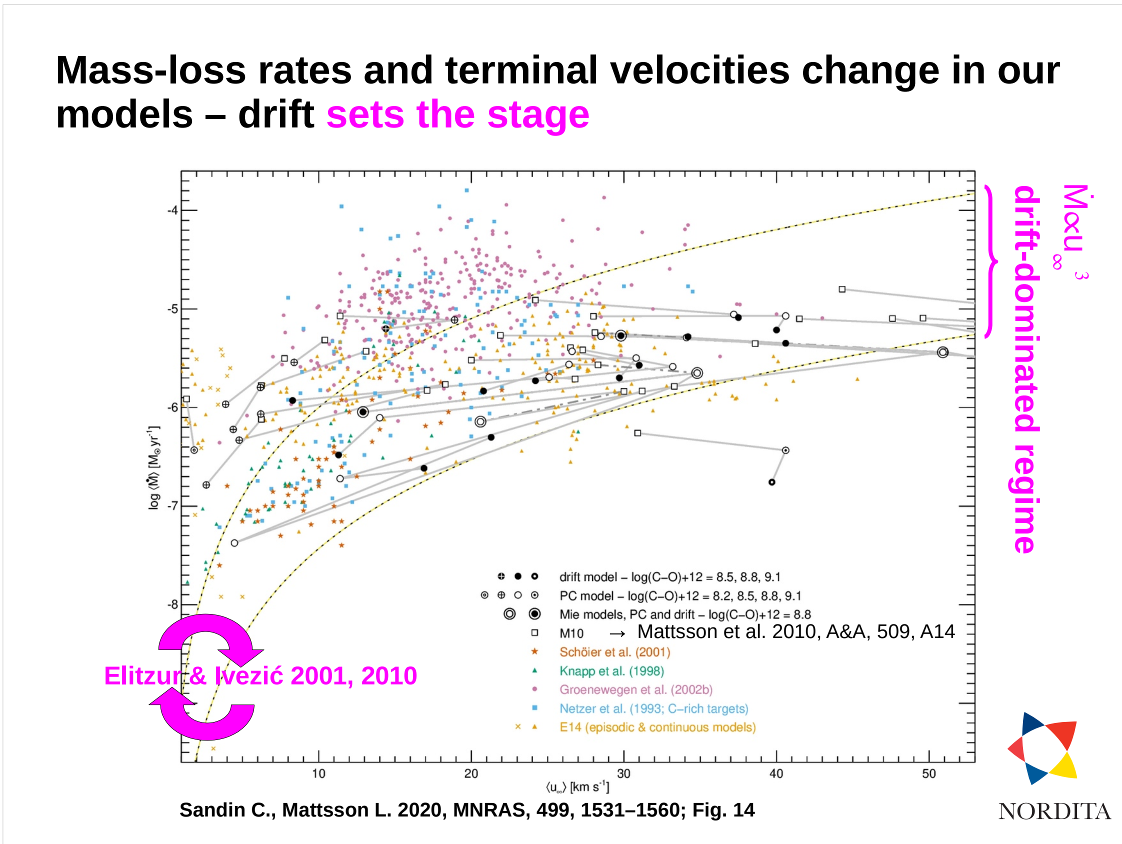

Here, we compare mean values of our C-rich models with other models and observations.

The plot shows mass loss rate (log of solar masses per year) versus terminal velocity (km/s).

The colored symbols show measurements of observations; the orange values are the model values of Eriksson et al. 2014.

Values of our models are shown with black symbols:

- a plus sign indicates the original value calculated by Mattsson et al. 2010...they use N_{grid}=100, N_ν=64, α=1.0.
- Black rings indicate our new PC model values...these are calculated using N_{grid}=1024, N_ν=319, α=~0.34.
- Black bullets indicate our drift models

Differences are significant, both between the two PC models and between our new PC models and the corresponding drift models

Changes between the values of Mattsson et al. 2010 and our new PC model values indicate that the numerical setup plays a role.

Note that nearly all our drift models are found in the optically thin ”drift-dominated region” as defined by Elitzur & Ivezić.

The wind formation efficiency is affected by drift, but also by the scattering approach

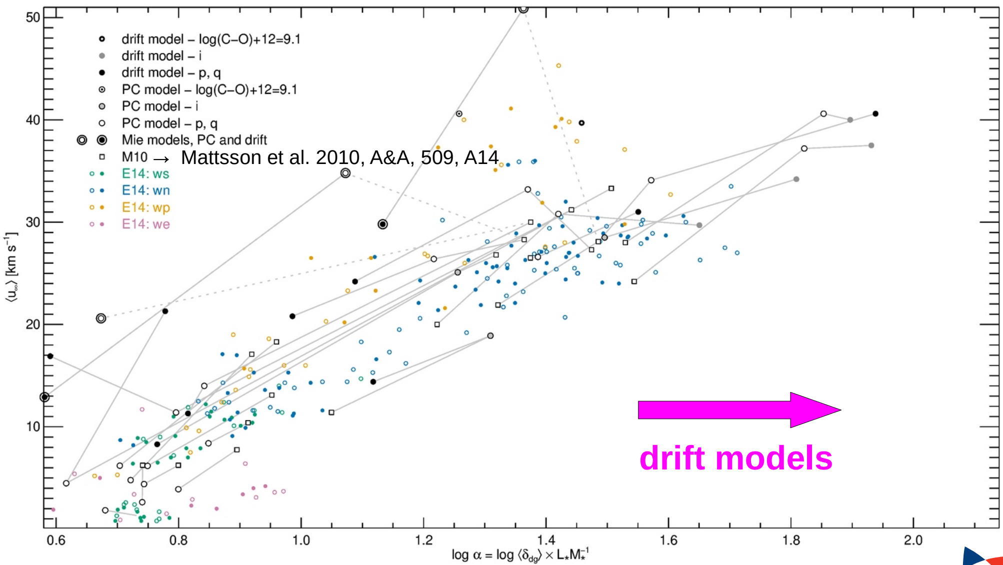

Sandin C., Mattsson L. 2020, MNRAS, 499, 1531–1560; Fig. 12

NORDITA

This plot shows the outflow velocity versus the α parameter, which is a measure for the wind-formation efficiency. (logarithmic axes!).

It appears that the drift models (black bullets) are all shifted to the left...and show a lower wind-formation efficiency paired with higher outflow velocities than the models of Eriksson et al. 2014.

But wait...<next slide>

The wind formation efficiency is affected by drift, but also by the scattering approach

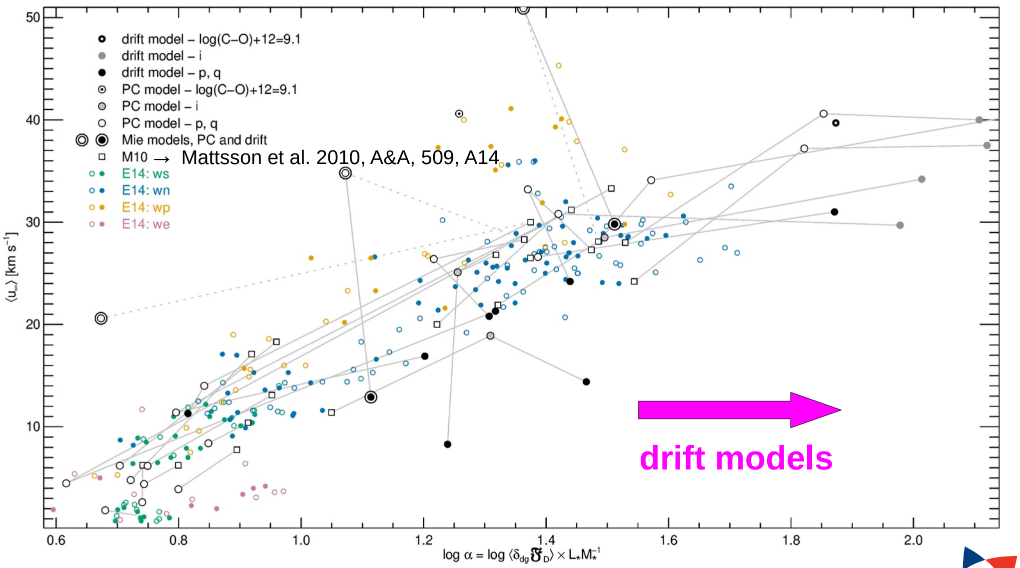

Sandin C., Mattsson L. 2020, MNRAS, 499, 1531–1560; Fig. 12

NORDITA

In comparison to earlier studies, we need to multiply the dust-to-gas density ratio with the drift factor (v/u) to get the correct amount of dust!

And now the group of drift models show a similar wind-formation efficiency as the PC models, at a somewhat lower expansion velocity.

But there is more...<next slide>

The wind formation efficiency is affected by drift, but also by the scattering approach

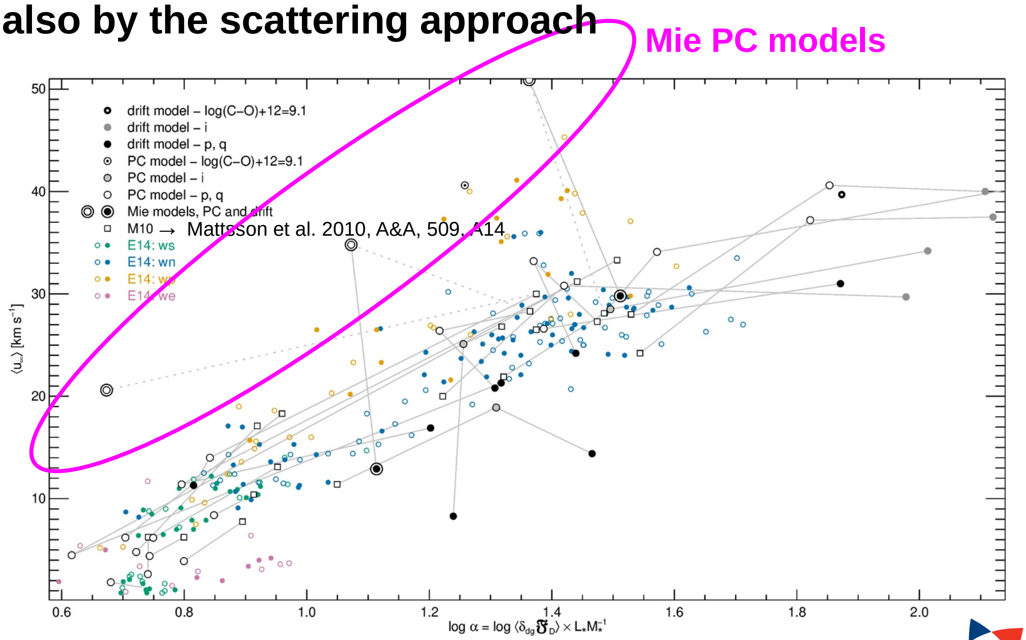

Sandin C., Mattsson L. 2020, MNRAS, 499, 1531–1560; Fig. 12

NORDITA

Also worth noting: PC models using Mie scattering are positioned above the other models at higher expansion velocities. When drift is used, these models join the other set of models.

It appears that using Mie theory to describe the dust opacity instead of the SPL – coupled with the higher numerical accuracy of our models where all shocks are resolved instead of a few – the models achieve a much higher outflow velocity than in the earlier models (Mattsson & Höfner 2011 didn't see anything like this).

It turns out that when we use Mie-theory instead of the SPL and relax the condition of PC models by allowing garins to drift, we solve an old and known problem of dust-driven winds. It has for a long time been believed that stellar winds of cool stars cannot be driven by dust as the outflow velocity becomes too high. By including drift, this problem is solved!

Plotting mass loss rates versus the drift factor

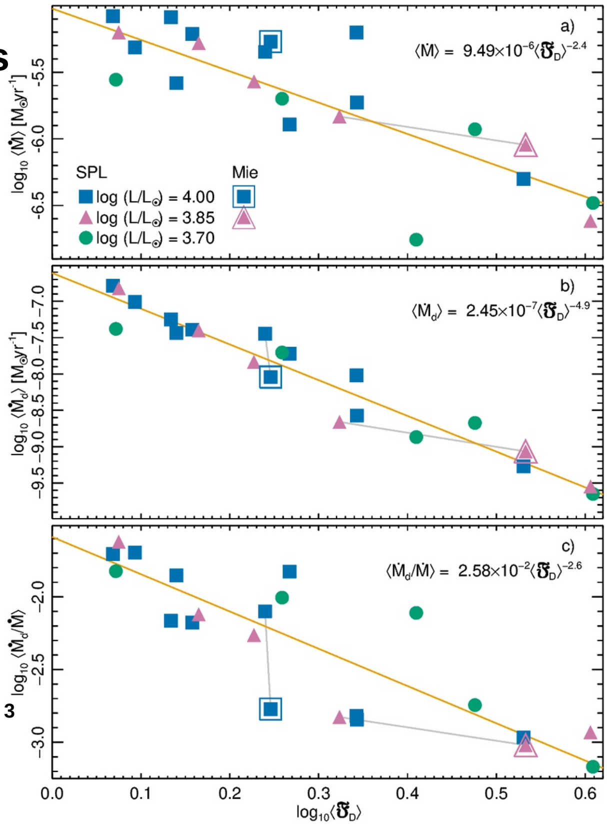

Sandin C., Mattsson L. 2020, MNRAS, 499, 1531–1560; Fig. 3

NORDITA

When we plot the various properties of the stellar wind models against the drift factor (F_D=v/u), we find an exponential dependence in most properties.

In particular, the dust mass loss rate is found to be most strongly correlated with the drift factor (middle panel in the figure).

The mass-loss rate of the gas (top panel) also shows something like an exponential dependence on the drift factor. Where higher mass-loss rates are found when there is no drift (left side) and the lowest mass-loss rates are found when the drift factor is the highest (right side).

The mass-loss rate is delimited by our models to about 10^{-7}–10^{-5} M_sun/yr.

These are all new relations that nobody else has the means to do – since no other model includes drift.

In conclusion: high spatial resolution, Mie-theory, and drift are all needed to understand the wind formation

4

Drift makes wind formation more difficult as dust can slip through the gas: lower expansion velocities

Drift also changes properties by a factor 50–1000%: more dust forms!

There is no reason that motivates excluding drift from realistic wind models of AGB stars

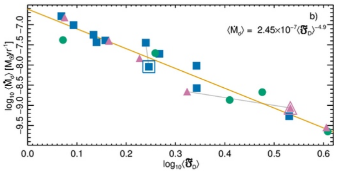

NORDITA

What you should take home from this talk is that existing results of stellar wind models can be improved, quite significantly!

In particular, by including drift, stellar wind models show lower expansion velocities – in line with observations. Additionally, the amount of dust is increased quite significantly, and in particular in models with a low mass-loss rate.

By including drift, stellar wind properties change drastically by about 50–1000%.

There is **no reason** to exclude drift in a realistic model of stellar winds on the asymptotic giant branch.

In conclusion: ...but we're not done yet, there are more physics improvements that should be addressed

The drag force depends on the grain size

The wind is a multi-component fluid

with one dust equation of motion per grain size (interval)

The dust CSE In the case of the dust, the challenges are considerable if the uncertainties in the dust-mass-loss-rate estimates, not to mention the conversion to the total mass-loss rate, are to be lowered well below the present order-of-magnitude level. The dust velocity cannot be measured, but possibly estimated with a good enough model for the dust acceleration. The dust composition must be determined, as well as the grain size distribution, and the structure of the grains (shape, coated, porous, etc.). This is a monumental task. As a reasonable step forward it would be of significant interest to study in detail the dust characteristics of the nearby sources that are well-studied in circumstellar CO. The estimated gas-mass-loss rates and gas terminal expansion velocities will provide important constraints on the dust modelling. This can serve as a very useful comparison sample for studies of mass loss in, e.g., extragalactic sources.

Höfner S., Olofsson H. 2018, A&ARv, 26, 1–92; page 72,
"7.1 Empirical mass loss rates: updates to the standard CSE model"

NORDITA

There are of course still aspects that can be improved.

One such aspect is that the stellar wind is actually not a three-component fluid but a multi-component fluid where grains of different size move at different velocities.

Our current wind models can with a relatively small effort be expanded to describe such multi-component fluids!

I show an excerpt from the recent AGB review paper, which towards the end mentions that we know very little about properties of the dusty circumstellar envelope (CSE).

In fact, with our models, we already can say something about the dust velocity in the CSE, and we could also, with a relatively small effort, calculate the grain size distribution.

Providing a good starting point in deciphering the dusty CSE!

Assumptions: accelerated dust grains drag gas particles through collisions – microscopic process

κ(gas), κ(dust), τ^{-1}, **drift**, RT

Increased grain formation with higher drift velocities!

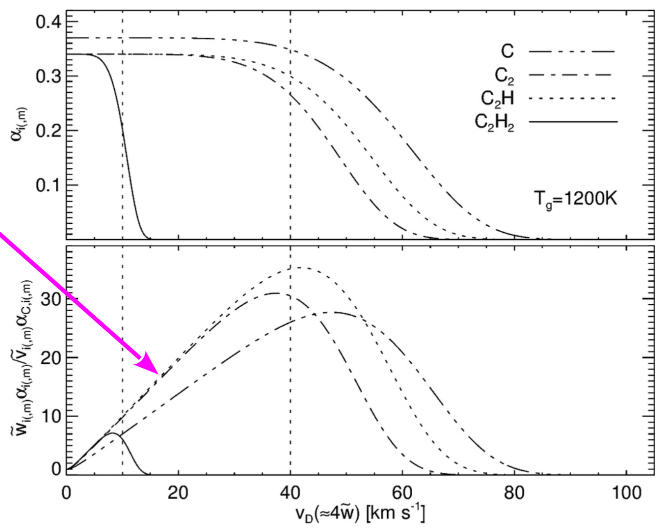

Sandin C., Höfner S. 2004, A&A 413, 789–798; fig. 1

NORDITA

Additional material (for possible questions):

The dust formation process depends on the drift velocity.

The upper panel shows how the sticking coefficient varies with the drift velocity; the binding energy is not enough to have impacting atoms and molecules stick at high drift velocities.

The most abundant molecule, C_2H_2, is also the molecule with the smallest binding energy.

The lower panel shows the net grain formation rate – the drift-velocity-dependent rate divided by the rate where the drift velocity is set to zero.

Obviously, the grain formation rate increases strongly also at low drift velocities; however, the increase stops at too high drift velocities where the sticking coefficient goes to zero.

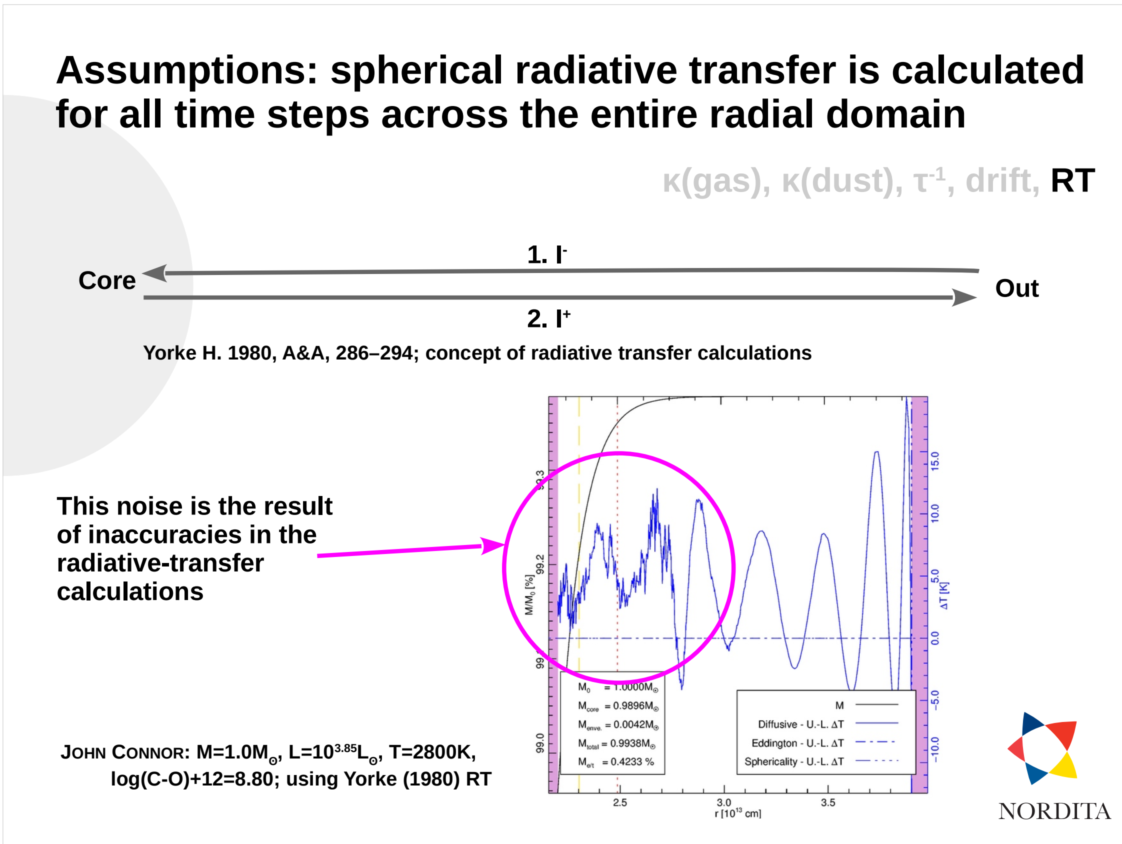

A good reason to replace the radiative-transfer solver of Yorke (1980) with a Feautrier-based solver is that the former shows problems due to numerical noise that the latter doesn't produce as easily.

The circled region shows temperature-correction values that result in one case during the creation of a hydrostatic initial model. The same noise **does not** appear when the model is instead calculated using a Feautrier-type solver.

Models using the formulation of Yorke show these issues sometimes, and not in all models.

Plotting remaining properties versus the drift factor

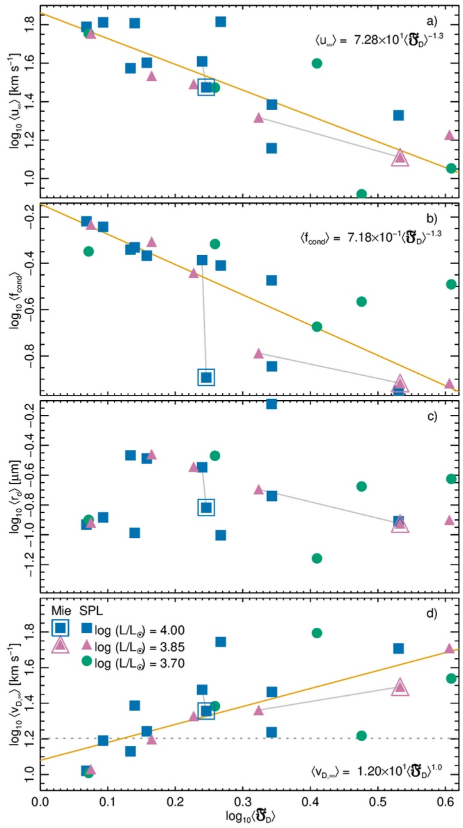

Sandin C., Mattsson L. 2020,
MNRAS, 499, 1531–1560; Fig. 5

NORDITA

This plot adds the remaining properties to the plot of the gas and dust mass-loss rates shown earlier.

All properties but the mean grain radius show an exponential dependence with the drift factor,

How numerical features appear in drift models in the form of spikes and troughs in the drift velocity

Sandin C., Mattsson L. 2020, MNRAS, 499, 1531–1560; Fig. 8, we use a mostly fixed grid

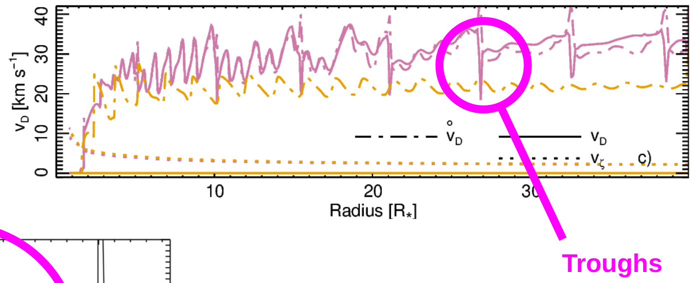

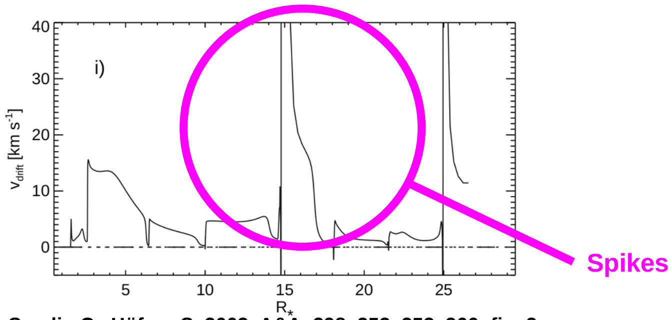

Sandin C., Höfner S. 2003, A&A, 398, 253, 253–266; fig. 2, we use the adaptive grid equation to resolve shocks

NORDITA

Understanding the numerical features in drift models

Starting with the work for my PhD thesis, I spent a dominant amount of my time trying to understand the spikes that I got in drift models.

I could not resolve the problem then, but I could mitigate their effect on the model convergence by adding some artificial diffusion. (The spikes hardly affected the physics of the models as they always appear where there is nearly no dust at all).

In out new models we do not use the adaptive grid equation to resolve shocks, and this removes the spikes. Instead we get something looking like ”troughs” in dust fronts.

(In the models of Sandin 2008 the spikes didn’t appear using the gray Planck-mean opacities. They seem to be ubiquitous in models that use a constant gas opacity and frequency-dependent gas opacities...which both have a higher density.)

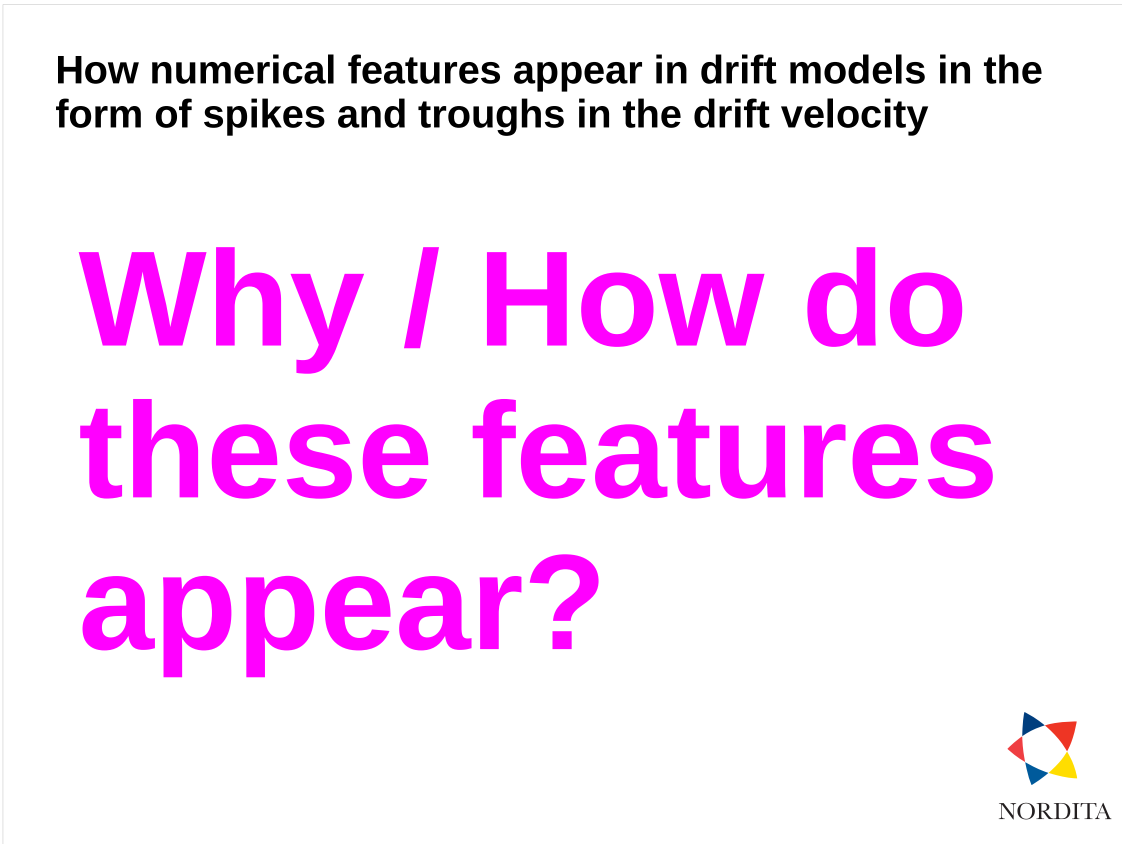

So, why do these features appear?

How numerical features appear in drift models in the form of spikes and troughs in the drift velocity

Volume weighted advection required with drift models!

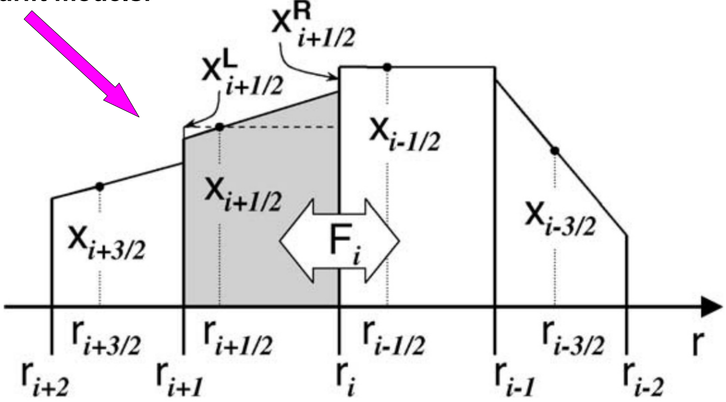

Dorfi E.A., Pikall H., Stökl A., Gautschy, A. 2006, Computer Physics Communications, 174, 771–782; fig. 2, introducing volume-weighted advection scheme

NORDITA

An important component is the, so-called, advection term that describes how mass, momentum, and energy is transported between cells.

Notably, current wind models require the volume-weighted advection scheme of Dorfi et al. 2006. This scheme makes the code work like a lubricated bike chain. Without it, the code works like a rusty chain, i.e. not at all.

How numerical features appear in drift models in the form of spikes and troughs in the drift velocity

$$\frac{\partial}{\partial t}(\rho_\mathrm{d} v) + \nabla \cdot (\rho_\mathrm{d} v\, v) = -\frac{G m_r}{r^2}\rho_\mathrm{d} + \frac{4\pi}{c}\chi_\mathrm{H} H + m_1 S v - f_\mathrm{drag}$$

advection term

i) Rewrite momentum advection using the integrated dust mass ($m_{d,r}$)

ii) Use advection scheme that accounts for ρ_d and *v* separately ⇒ Vanderheyden & Kashiwa 1998, J. Comp. Phys., 146, 1

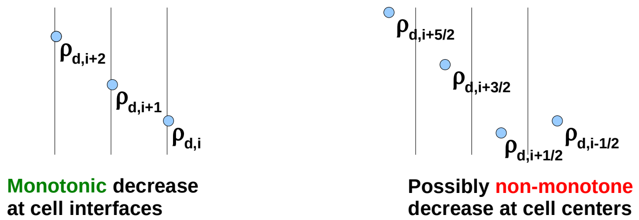

NORDITA

The root of the problem of spikes in the dust velocity is isolated to the advection term in the dust equation of motion.

In PC models, one can rewrite the advection of gas momentum using the integrated mass equation. Thereby the momentum – density times velocity – is replaced with a temporal difference of the integrated mass. This works great in PC models!

In drift models, one can do this as well. One adds an equation describing the integrated dust mass, and uses that to advect the dust momentum. We have tried this approach and it doesn't work. Probably because the integrated dust mass is too imprecise.

We noted however, that the advection of the momentum can be re-formulated using an approach developed by Vanderheyden and Kashiwa 1998. In their approach, the density and velocity are delimited separately...lowering the cell slope order to 0 when the slope is not monotone.

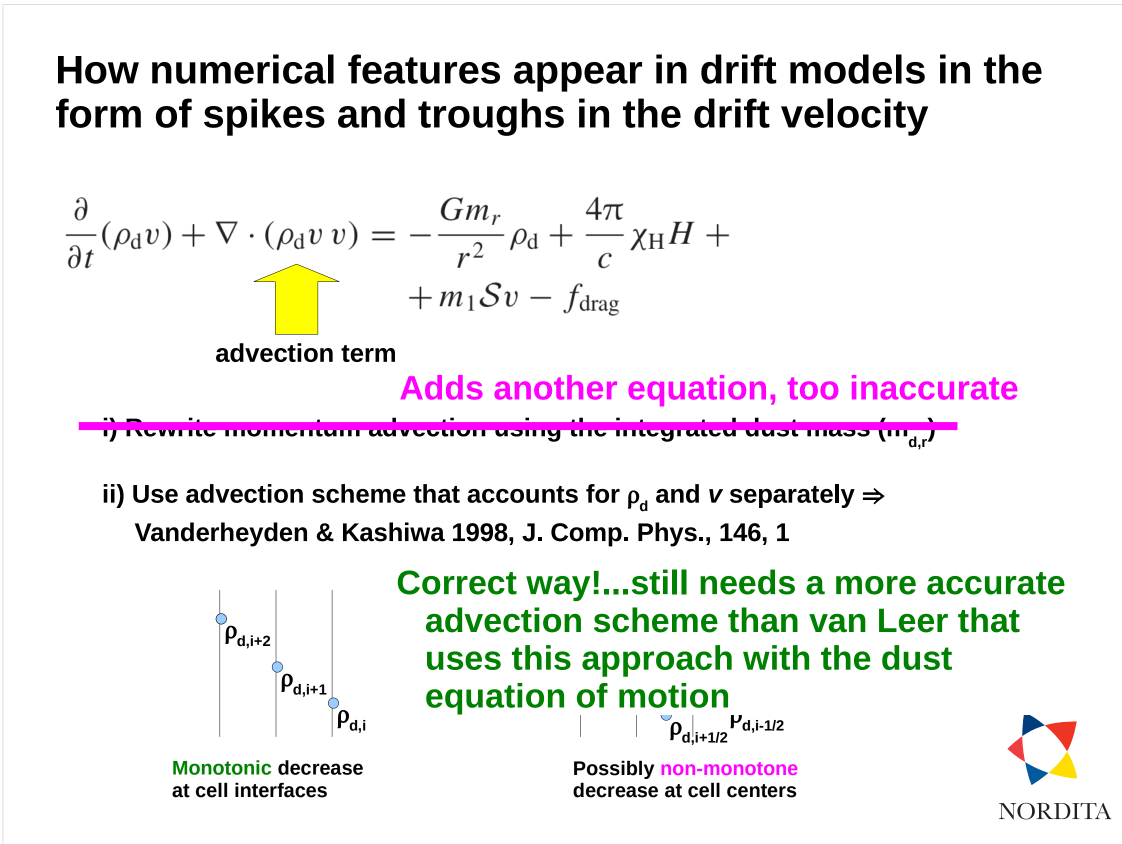

And this does indeed explain the problem!

In our models that use a so-called staggered mesh, densities are placed at cell centers while velocities are placed at cell boundaries.

What is necessary is an advection scheme where the density is delimited at cell centers before they are combined with velocities that are delimited at cell boundaries.

The scheme of Vanderheyden & Kashiwa 1998 is a first step, but it needs to be enhanced with the volume-weighted formulation of Dorfi et al. 2006 to work with our drift models.

We have begun the work to achieve this, and this work is still on-going.